JOC The Journal of Organic Chemistry

Article

pubs.acs.org/joc

Bicarbazoles: Systematic Structure–Property Investigations on a Series of Conjugated Carbazole Dimers

Shin-ichiro Kato, Hiroto Noguchi, Atsushi Kobayashi, Toshitada Yoshihara, Seiji Tobita, and Yosuke Nakamura*

Department of Chemistry and Chemical Biology, Graduate School of Engineering, Gunma University, 1-5-1 Tenjin-cho, Kiryu, Gunma 376-8515, Japan

Supporting Information

ABSTRACT: A large series of conjugated carbazole dimers, namely bicarbazoles **1**–**12**, were synthesized by Suzuki–Miyaura, Sonogashira, Hay, and McMurry coupling reactions. In **1**–**12**, the two carbazole moieties are linked at the 1-, 2-, or 3-position directly or via an acetylenic or olefinic spacer. The structure–property relationships, particularly the effects of the conjugation connectivity and the π-conjugated spacers on the electronic, photophysical, and electrochemical properties of **1**–**12**, were studied by extensive UV–vis and fluorescence spectroscopic measurements, cyclic voltammetry (CV), and theoretical calculations as well as X-ray crystallographic analyses. The connection at the 1-position of carbazole ensures high extent of π-conjugation, while that at the 3-position enhances the electron-donating ability. Both acetylenic and olefinic spacers allow the extension of π-conjugation, and the latter also causes the increase of the donor ability. Moreover, the structural variations were found to affect the fluorescence quantum yields significantly, which are up to 0.84.

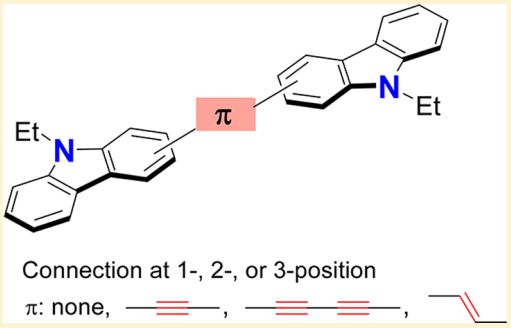

INTRODUCTION

Carbazole with fine optical and electronic properties and high chemical stability has found wide applications in functional materials.[1] Oligo-/polycarbazoles have been representative materials in organic light-emitting diodes (OLEDs),[2,3] organic field-effect transistors (OFETs),[4] and organic photovoltaics (OPVs),[5] to date. Poly(3,6-carbazole)s and 3,6-functionalized carbazole derivatives were extensively studied because carbazole can be easily functionalized by electrophilic aromatic substitution at its 3,6-positions (*para* positions from the nitrogen atom) with high electron density.[1,6] The nitrogen atom of the carbazole moiety can be also functionalized by alkylation or arylation reaction, and thereby the solubility and other properties of polymers and oligomers can be properly controlled. The efficient synthetic pathways to poly(2,7-carbazole)s and 2,7-functionalized carbazole derivatives have been established in the past decade,[7] and their peculiar properties which are apparently different from those of 3,6-carbazole derivatives, and their potential applications have been explored by Leclerc and co-workers.[1b−d] When the 3,6-positions of carbazole are first protected, the 1,8-positions (*ortho* positions from the nitrogen atom) can be readily functionalized because they are also activated.[8,9] Very recently, Michinobu and co-workers first synthesized 1,8-linked carbazole polymers with acetylenic spacers and demonstrated their interesting opto-electronic properties.[10]

The systematic study on oligomers with precisely defined length, constitution, and conformation allows the elucidation of correlation of physicochemical properties with chemical structures, enables the generation of useful and predictable structure–property relationships, and sheds light on the properties of polymers.[11] In the molecular design of oligomers for their applications into π-functional materials, the π-conjugated spacers have to be carefully chosen to achieve the desired properties, because they play a crucial role in the physicochemical properties, such as photophysical and electrochemical properties, and spread of frontier molecular orbitals (FMOs). Popular π-spacers in conjugated oligomers comprise C=C double bonds, C≡C triple bonds, and mixed eneyne systems, which ensure high planarity of the molecules and thereby allow the efficient π-conjugation.

The ongoing quest for carbazole-based electronic and opto-electronic materials has stimulated much structural variation, in particular, the insertion of π-conjugated spacers between carbazole moieties as well as the modification of conjugation connectivity. Strohriegl and co-workers reported in 1994 the first example of structurally well-defined 3,6-carbazole oligomers, namely dimer and trimer, in which the carbazole moieties are linked by ethynylene spacers.[12a] Recently, Lu, Liu, Wang, and co-workers synthesized 3,6-carbazole pentamer and hexamer[13] and demonstrated that they function as hole-transporting materials in OLED devices.[13a] The directly connected 3,6-carbazole and 2,7-carbazole oligomers were also exploited by Strohriegl and co-workers, and their glass transition temperature and hole-drift mobility were inves-

Received: August 7, 2012
Published: September 17, 2012

dx.doi.org/10.1021/jo3016538 | J. Org. Chem. 2012, 77, 9120–9133

Chart 1

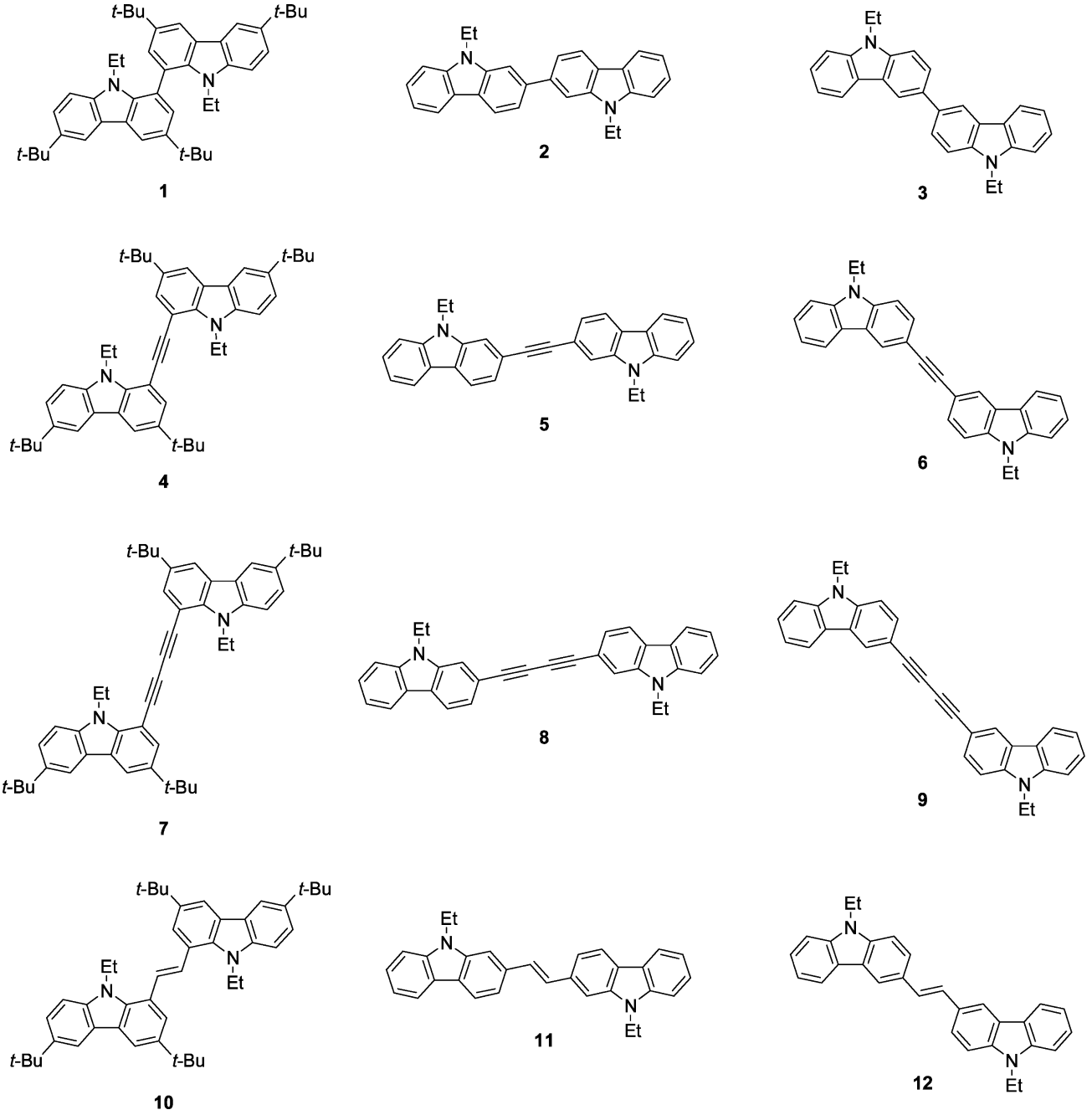

tigated.[12b,c] The 3,6-carbazole dimers with an ethenylene spacer were independently reported by Lin and co-workers[14a] and Xu, Liu, Zhu, and co-workers.[14b] The latter group also prepared the macrocyclic carbazole dimer connected by ethenylene spacers and demonstrated that the OFET devices based on the macrocycle showed the hole mobility as high as 0.013 $cm^2 V^{-1} s^{-1}$.[14b] Meanwhile, Leclerc and co-workers synthesized the 2,7-carbazole trimers connected by ethenylene spacers as p-type semiconducting materials.[15] Although various carbazole oligomers have been reported as summarized above, almost no systematic study focusing on the effects of the conjugation connectivity and the π-spacers in carbazole oligomers on their fundamental properties, such as the optical and electrochemical properties, has been reported so far, to the best of our knowledge. Notably, the synthesis of 1,8-carbazole oligomers is completely lacking. In this context, we became interested in conjugated carbazole dimers, namely bicarbazoles **1**−**12**, in which the two carbazole moieties are linked at the 1-, 2-, or 3-position directly or via an ethynylene, butadiynylene, or ethenylene spacer (Chart 1). The comprehensive study on physicochemical properties of a large series of bicarbazoles **1**−**12** should allow us to establish the general and useful structure−property relationships of conjugated carbazole π-systems.[16] Here, we wish to report the synthesis, the structural features, and the electronic, photophysical, and redox properties of **1**−**12** on the basis of X-ray crystallographic analyses, UV−vis and fluorescence spectroscopies, cyclic voltammetry, and theoretical calculations.

dx.doi.org/10.1021/jo3016538 | J. Org. Chem. 2012, 77, 9120−9133

Scheme 1. Synthesis of 1 and 2

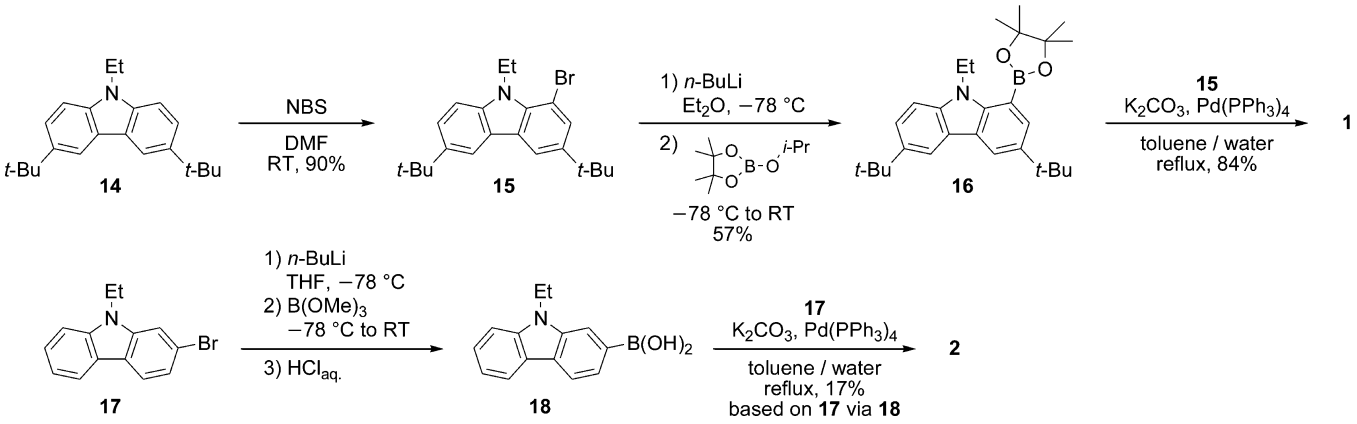

Scheme 2. Synthesis of 4–6

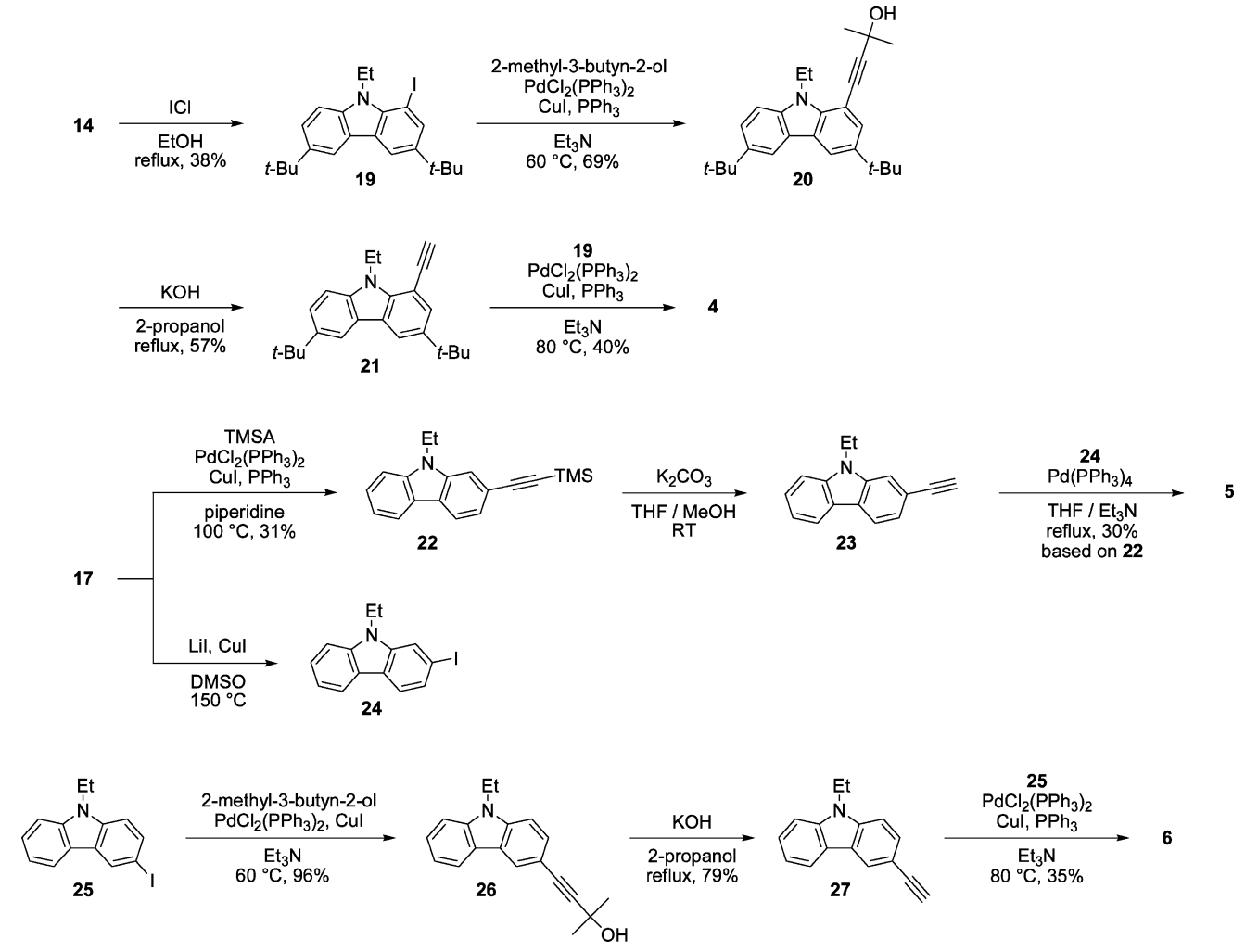

RESULTS AND DISCUSSION

Synthesis. Compounds **3**[17] and **12**[14] are known in the literature. To functionalize the 1,8-positions of the carbazole moiety, *tert*-butyl groups were first introduced at the 3,6-positions in **1**, **4**, **7**, and **10** by Friedel–Crafts alkylation reactions with 2-chloro-2-methylpropane in the presence of $ZnCl_2$ catalyst. Bicarbazoles **1** and **2** were synthesized by Suzuki–Miyaura coupling reactions as key steps (Scheme 1).[18] Bromination of **14** with 1 equiv. of NBS afforded **15** in high yield, which was readily converted to boronic acid pinacol ester **16** via lithiation with *n*-BuLi in THF followed by the treatment with 2-isopropoxy-4,4,5,5-tetramethyl-1,3,2-dioxaborolane. Compound **1** was obtained in 84% yield by the Suzuki–Miyaura coupling reaction of bromide **15** and **16** with $Pd(PPh_3)_4$ as catalyst. By the similar cross-coupling procedure, **2** was synthesized. Thus, 2-bromo-*N*-ethylcarbazole (**17**) was

dx.doi.org/10.1021/jo3016538 | J. Org. Chem. 2012, 77, 9120–9133

converted into boronic acid **18**, which was then subjected to the Suzuki–Miyaura reaction with bromide **17** to afford **2**.

The synthesis of bicarbazoles **4**–**6** relies on Pd-catalyzed Sonogashira cross-coupling reactions as key steps (Scheme 2).[19] The Sonogashira reaction of monoiodide **19** obtained by iodination of **14** with ICl and 2-methyl-3-butyn-2-ol gave **20**. The deprotection of **20** with KOH in 2-propanol readily afforded **21**. The Sonogashira coupling reaction of **21** and **19** gave **4** in 40% yield. For the synthesis of **5**, compound **23** was synthesized by the Sonogashira reaction of **17** and trimethylsilylactylene (TMSA) followed by the removal of TMS group with K_2CO_3. The Sonogashira reaction of **23** and **17**, however, produced no desired **5**, and homocoupling product **8** was obtained. Therefore, bromide **17** was converted to iodide **24** with excess amounts of CuI/LiI in DMSO.[20,21] The reaction of **23** and **24** with $Pd(PPh_3)_4$ catalyst and CuI cocatalyst was first examined, but **8** was again isolated exclusively.[22] Finally, when $Pd(PPh_3)_4$ was employed as the sole catalyst in the absence of CuI,[23] the homocoupling reaction of **23** was suppressed to some extent and **5** was obtained. Similar to the synthetic route of **4**, bicarbazole **6** was prepared in 3 steps from **25**. The synthesis of **7**, **8**, and **9** was readily accomplished by oxidative homocoupling reactions of terminal alkynes **21**, **23**, and **27**, respectively, by Hay coupling reactions with CuCl and *N*,*N*,*N*′,*N*′-tetramethylethylenediamine (TMEDA) in toluene (Scheme 3).[24]

Scheme 3. Synthesis of 7–9

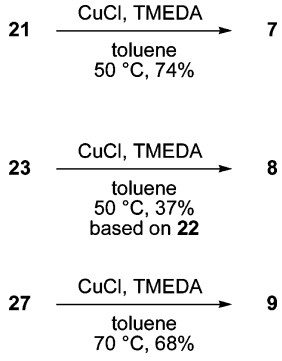

Similar to the synthesis of **12** described in the literature,[14] the preparation of **10** and **11** relies on McMurry coupling reactions (Scheme 4).[25] Thus, lithium–bromine exchange between **15** and *n*-BuLi followed by the successive addition of piperidine-1-carbaldehyde and aqueous NH_4Cl gave aldehyde **28**, which was allowed to react with $TiCl_4$ and zinc powder in THF to furnish **10** in 78% yield. Similarly, **11** was prepared from aldehyde **29** by employing the slightly modified reaction conditions. All of the compounds were fully characterized by various spectroscopic methods, such as ^1H NMR, ^{13}C NMR, and mass spectroscopy and/or elemental analysis.

Scheme 4. Synthesis of 10 and 11

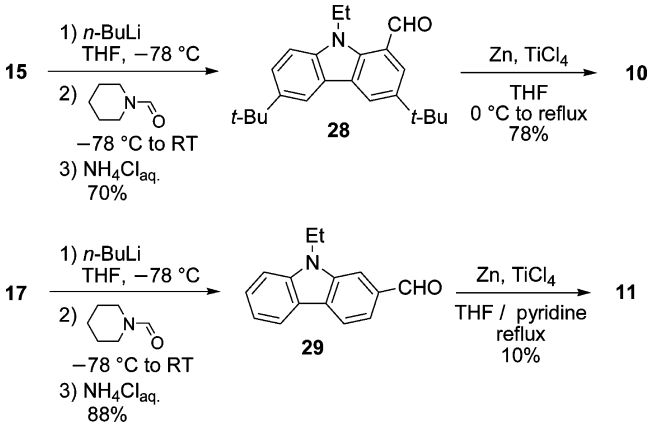

Structural Properties. The single crystals of **2**, **4**, and **10** suitable for X-ray diffraction analyses were obtained by vapor diffusion of hexane into CH_2Cl_2 solution of the molecules (Figure 1). The two carbazole moieties in **2** are twisted from each other with the dihedral angle for C26–C15–C10–C11 of −25.2°. On the other hand, the dihedral angles for C12–C11–C25–C26 in **4** and C10–C11–C11′–C12′ in **10** are only −3.8° and 1.7°, respectively. Thus, the introduction of π-spacers between the two carbazole moieties apparently results

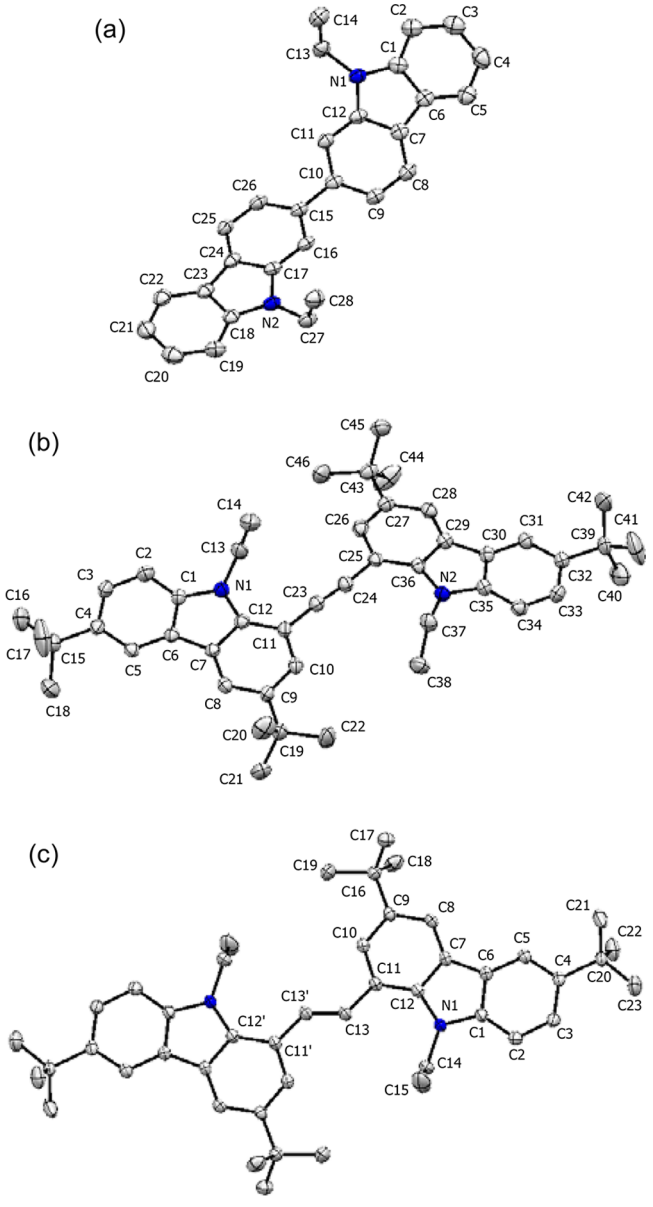

Figure 1. ORTEP plots of (a) **2**, (b) **4**, and (c) **10** with displacement ellipsoids at 50% probability level. Arbitrary numbering; hydrogen atoms are omitted for clarity.

dx.doi.org/10.1021/jo3016538 | J. Org. Chem. 2012, 77, 9120–9133

Table 1. Optical Data and Calculated Lowest Excitation Energies of 1−12

	λ_{max} [nm][a]	λ_{onset} [nm][b]	λ_{fl} [nm][a]	Φ_f[c]	calcd λ_{max} [nm] (f)[d]	composition of band[d]
1	269, 301, 342, 356	370	369, 380	0.52	318 (0.010)	H−3→L+3, 3%; H−2→L+2, 3%; H−1→L+1; 22%, H→L, 63%
2	267, 326, 350[e]	375	375[e] 398	0.84	331 (0.111)	H−2→L, 74%; H−1→L+1, 2%, H→L, 11%; H→L+3, 3%
3	265,[e] 303, 345,[e] 360[e]	370	395[e] 413, 440[e]	0.18	328 (0.039)	H−2→L+2, 5%; H−2→L. 2%, H→L+1, 86%
4	260,[e] 279, 306, 345,[e] 384, 400	415	412, 435,[e] 450[e]	0.81	389 (0.599)	H→L, 96%
5	265, 280,[e] 320,[e] 343, 369	385	386, 401	0.80	366 (1.776)	H→L, 85%
6	276, 305, 323, 340,[e] 350,[e] 365[e]	380	378, 393	0.60	344 (0.216)	H−2→L+2, 2%; H→L, 67%; H→L+2, 19%
7	290,[e] 303, 330,[e] 394, 412	435	431, 475[e]	0.22	409 (0.839)	H→L, 95%
8	264, 305,[e] 340,[e] 354, 382	405	399, 416, 430[e]	0.21	395 (1.956)	H−4→L+2, 3%; H→L, 96%
9	280,[e] 299, 342, 360, 372	390	384, 415[e]	0.002	371 (1.635)	H−4→L+3, 5%; H→L, 94%
10	270,[e] 303, 378	430	447, 470,[e] 515[e]	0.83	376 (0.538)	H→L, 96%
11	267, 285,[e] 368, 385[e]	415	411, 423	0.59	376 (1.906)	H→L, 98%
12	270,[e] 300,[e] 308, 342, 370,[e] 395[e]	410	411, 430[e]	0.63	355 (0.689)	H−2→L, 2%; H→L, 65%; H→L+2, 30%

[a]In CH_2Cl_2. [b]The longest energy absorption wavelengths with a molar absorptivity (ε) = 1000 L mol^{-1} cm^{-1} for **1**−**12** and 500 L mol^{-1} cm^{-1} for **13** and **14**. [c]Absolute quantum yields determined by an integrating sphere system in cyclohexane. [d]TD-DFT (TD/B3LYP/6-31G*) calculations were carried out with use of optimized structures at B3LYP/6-31G* level of theory, and only energies with f > 0.01 are shown; f = oscillator strength; H = HOMO, L = LUMO. [e]Peak as shoulder.

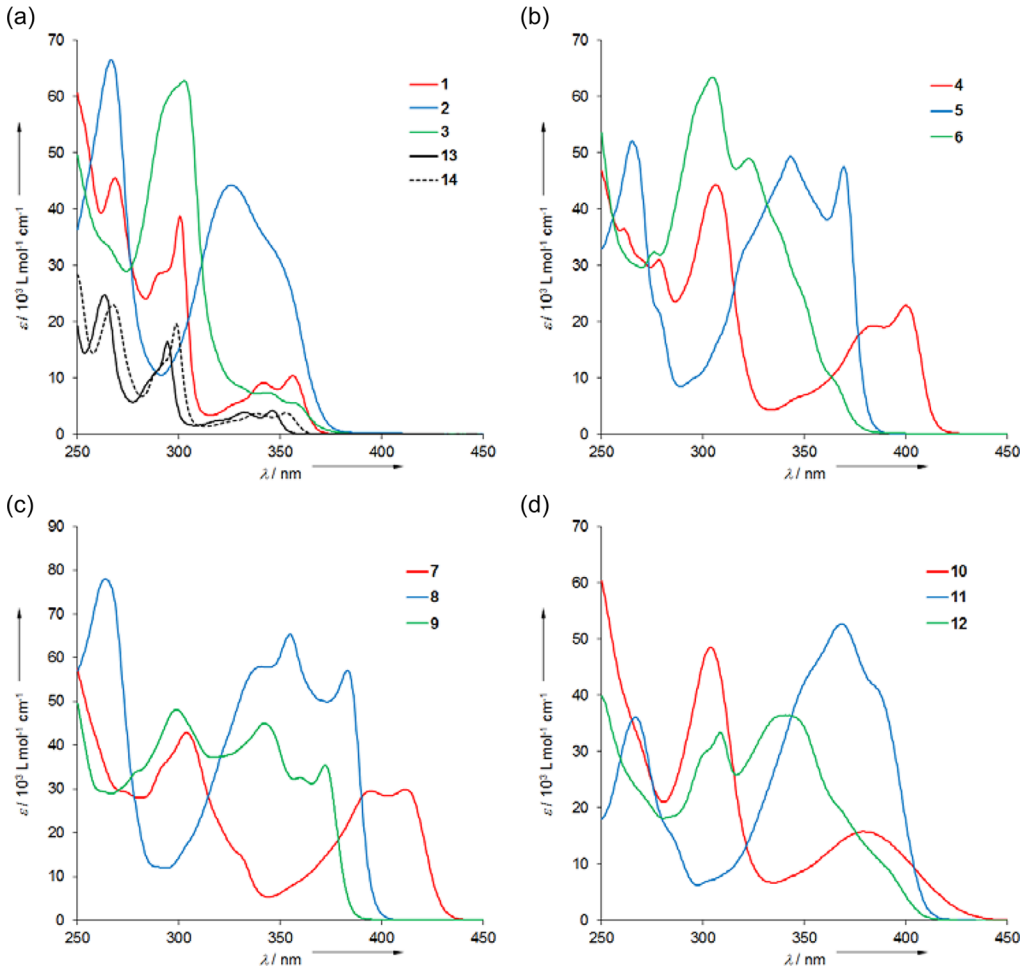

Figure 2. Electronic absorption spectra of (a) **1**−**3**, **13**, and **14**, (b) **4**−**6**, (c) **7**−**9**, and (d) **10**−**12** in CH_2Cl_2 at room temperature.

in high planarity of the molecules, and thereby should lead to the effective extension of π-conjugation (*vide infra*). In all of **2**, **4**, and **10**, molecules are packed via multiple CH−π interactions, and almost no characteristic cofacial intermolecular interaction is observed.

To gain further insight into the molecular structures, we optimized the ground-state structures of **2**, **4**, and **10** by density functional theory (DFT) calculations at the B3LYP/6-31G* level of theory without any symmetry constrains by Gaussian 03 suit of program.[26] The selected geometrical parameters of **2**, **4**, and **10** are summarized in Supplementary Tables S1−S3

dx.doi.org/10.1021/jo3016538 | J. Org. Chem. 2012, 77, 9120−9133

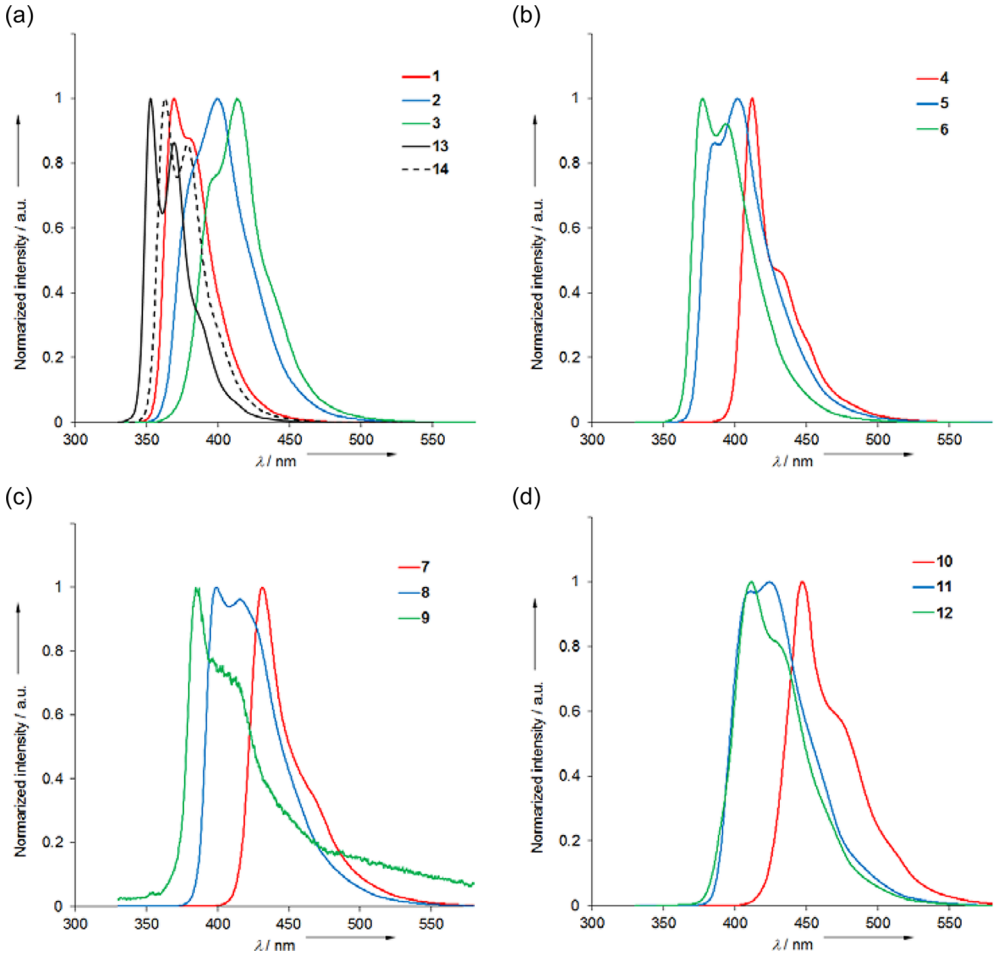

Figure 3. Fluorescence spectra of (a) **1**–**3**, **13**, and **14**, (b) **4**–**6**, (c) **7**–**9**, and (d) **10**–**12** on 320-nm excitation in CH_2Cl_2 at room temperature.

(Supporting Information) and compared with the crystallographic dihedral angles and bond lengths. Regarding the bond lengths, there is good agreement between the experiments and theory. Thus, the differences for the C–C bond lengths and the C–N bond lengths are mostly within 0.016 Å. Exceptionally, the C=C bond length in **10** obtained by DFT calculations is longer than the crystallographic bond length by 0.027 Å. The dihedral angles between the two carbazole moieties for **2**, **4**, and **10** are estimated to be −38.0°, −23.1°, and 10.2°, respectively, and hence the DFT calculations gave distinctly larger angles than those in the X-ray results by ca. 10–20°. Crystal packing force may contribute to the observed high planarity of **2**, **4**, and **10** in the solid state.[27]

Electronic Absorption Spectroscopy. We measured the UV–vis spectra of **1**–**12** as well as *N*-ethylcarbazole (**13**) and 3,6-di-*tert*-butyl-*N*-ethylcarbazole (**14**) in CH_2Cl_2 and the data are summarized in Table 1. It is noteworthy that the extent of π-conjugation of bicarbazoles is highly dependent on the conjugation connectivity and the π-conjugated spacers as described below.

Bicarbazole **1** exhibits a quite similar absorption curve to that of **14** and has almost twice as large molar extinction coefficient (ε) as **14**, indicating that steric hindrance enforces almost no π-conjugation between the two carbazole moieties in **1** (Figure 2a). Thus, the marked twist around the C–C bond connecting the two carbazole moieties in **1** as a result of steric hindrance of the two ethyl groups should make its π-conjugation insufficient. Bicarbazoles **2** and **3** display clearly different absorption curves from that of **13**, reflecting the extension of π-conjugation, and the absorption onset (λ_{onset}) of **2** is bathochromically shifted relative to that of **3** (375 nm (**2**), 370 nm (**3**)). These results confirm that the connection at the 2-position of carbazole is more effective for the extension of π-conjugation than that at the 3-position when the two carbazole moieties are connected directly. The ε values of **2** in the longer wavelength region are quite large as compared to that of **3**.

The moderate bathochromic shifts of the longest absorption maxima (λ_{max}) and λ_{onset} are observed in **5** and **6** compared with **2** and **3**, respectively, by ca. 10–20 nm owing to the extension of π-conjugation as a result of the introduction of the ethynylene spacer in **5** and **6** (Figure 2b). Interestingly, the ethynylene linkage in **4** brings about a remarkable bathochromic shift of the longest λ_{max} in comparison to **1** by ca. 50 nm, which should reflect the release of twist and the resulting effective π-conjugation. As a consequence, in the series of **4**–**6**, compound **4** features the most red-shifted λ_{max} (400 nm (**4**), 369 nm (**5**), 365 nm (**6**)). Noticeably, the ethynylene spacer in **4** and **6** increases the ε values in the longer wavelength region. Compounds **7**–**9** feature the red-shifted longest λ_{max} and λ_{onset} by 7–20 nm as compared to the corresponding **4**–**6**, demonstrating that the elongation of the acetylenic spacer leads to further extension of π-conjugation as shown in Figure 2c (412 nm (**7**), 382 nm (**8**), 372 nm (**9**)). As compared to **4**–**6**, the corresponding **10**–**12** having an ethenylene linkage display bathochromically shifted λ_{onset} values by 15–30 nm (430 nm (**10**), 415 nm (**11**), 410 nm (**12**)). It is clear that the

dx.doi.org/10.1021/jo3016538 | J. Org. Chem. 2012, 77, 9120–9133

conjugation of bicarbazole π-systems is effectively extended by the ethenylene spacer than the ethynylene spacer.[28] Moreover, the λ_{onset} values of **11** and **12** are found to be somewhat red-shifted relative to those of **8** and **9**, respectively, while the λ_{onset} of **10** is slightly blue-shifted relative to **7** (Figure 2d).

Importantly, the effect of the conjugation connectivity of the two carbazole moieties on the extent of π-conjugation, that is the HOMO−LUMO gap, is clearly visible in the absorption spectra of the series of **4**−**6**, **7**−**9**, and **10**−**12**. In each series, the connection at the 1-position of carbazole leads to the most red-shifted λ_{onset}, and that at the 3-position leads to the least. The reason why **1** provides the most blue-shifted λ_{onset} in the series of **1**−**3** is the significant nonplanarity of **1** as compared to **2** and **3**[29] discussed above. Overall, it is likely that flat bicarbazole π-systems, such as **2**, **4**, and **10** as confirmed by the X-ray analyses, essentially obey the established trend of the conjugation connectivity for the extent of π-conjugation irrespective of the π-spacers: 3- < 2- < 1-positions, although we cannot entirely rule out the effect of *t*-Bu groups in **1**, **4**, **7**, and **10** on their absorption spectra.[30]

Fluorescence Spectroscopy. All the compounds in the present study are fluorescent. We performed the fluorescence spectral measurements by using the diluted CH_2Cl_2 solution (10^{-5}−10^{-6} mol/L), and the spectral data are summarized in Table 1. The color of the fluorescence of bicarbazoles ranges from violet, blue, to light green (Figure 3). As is the case with the λ_{max} values of **1**−**12**, their emission maxima (λ_{fl}) are generally dependent on the conjugation connectivity of the two carbazole moieties. Thus, the trend of the 3- < 2- < 1-positions in order of increasing λ_{fl} values holds for **4**−**12**. For instance, **4**, **5**, and **6** feature emission with the λ_{fl} of 412 nm, 386 nm, and 378 nm, respectively. Compounds **1**−**3** have slightly different trend, and thus **3** displays the red-shifted λ_{fl} relative to **1** and **2** by approximately 20 nm (369 nm (**1**), 375 nm (**2**), 395 nm (**3**)). The insertion of π-spacers between the two carbazole moieties results in the bathochromic shifts of λ_{fl}, and the ethenylene spacer has the pronounced effect as compared to the ethynylene and butadiynylene spacers. Consequently, the observed λ_{fl} of 447 nm in **10** is the longest among the compounds in this study. It is uncertain at present why the λ_{fl} of **3** is at somewhat longer wavelength than **6** and **9**.

We determined the absolute fluorescence quantum yields (Φ_f) of **1**−**12** by an integrating sphere system (Table 1).[31] The conjugation connectivity of carbazole and the conjugated spacers also affect the Φ_f values significantly. The Φ_f values of **1**, **2**, and **3** are 0.52, 0.84, and 0.18, respectively. The introduction of the ethynylene spacer increases the Φ_f values as found in **4**−**6**. Thus, **4** and **6** display the Φ_f values of 0.81 and 0.60, respectively, which are higher than those of **1** and **3**, respectively, and **5** also exhibits high Φ_f value of 0.80 comparable to that of **2**. Again, the ethenylene spacer ensures high Φ_f values as observed in **10**−**12**. Hence, the Φ_f values of **10** and **12** are almost equal to those of **4** and **6**, respectively, whereas the Φ_f value of **11** (0.59) is slightly decreased relative to that of **5**. The extension of the acetylenic spacer from **4**−**6** to the corresponding **7**−**9** results in significant decrease of their Φ_f values. Bicarbazoles **7** and **8** show the Φ_f values of 0.22 and 0.21, respectively, which are almost one-third of those of **4** and **5**, respectively, and the lowest Φ_f value was observed in **9** to be 0.002. It is worth mentioning that **2**, **4**, **5**, and **10** display the remarkably high Φ_f values over 0.80, which are almost two times as high as that (ca. 0.4) of parent **13**.[32] These results clearly demonstrated that the appropriate connection of carbazole moieties directly or via π-conjugated spacers enhances Φ_f values. It is likely that the connection at the 1- and 2-positions of carbazole are generally responsible for higher Φ_f values than that at the 3-position.

Electrochemistry. In order to elucidate the effects of the conjugation connectivity and the π-spacers in bicarbazoles on the donor ability, that is the HOMO level, experimentally, we performed the cyclic voltammetry (CV) for **1**−**12** as well as **13** and **14** in CH_2Cl_2 containing 0.1 mol/L *n*-Bu_4NPF_6 as the supporting electrolyte. The oxidation potentials (E_{pa}) versus Fc^+/Fc (ferrocenium/ferrocene couple) are listed in Table 2.

Table 2. Oxidation Potential (E_{pa}) by Cyclic Voltammetry in CH_2Cl_2 (0.1 mol/L *n*-Bu_4NPF_6),[a] Theoretically Calculated HOMO and LUMO Levels and their Gaps ($\Delta E_{HOMO-LUMO}$),[b] and Optical HOMO−LUMO Gaps (ΔE_{opt})[c]

	E_{pa} [V]	HOMO [eV]	LUMO [eV]	$\Delta E_{HOMO-LUMO}$ [eV]	ΔE_{opt} [eV]
1	+0.70[d]	−5.40	−1.00	4.40	3.35
	+0.93[d]				
2	+0.74[e]	−5.48	−1.36	4.12	3.30
3	+0.46[d]	−5.15	−0.98	4.17	3.35
	+0.84[d]				
4	+0.57[d]	−5.11	−1.57	3.54	2.99
	+0.87[d]				
5	+0.77[e]	−5.35	−1.70	3.65	3.22
6	+0.51[e]	−5.05	−1.07	3.98	3.26
7	+0.68[d]	−5.23	−1.81	3.42	2.85
	+0.86[d]				
8	+0.91[e]	−5.39	−1.95	3.44	3.06
9	+0.67[e]	−5.12	−1.41	3.71	3.18
10	+0.49[d]	−5.12	−1.43	3.69	2.88
	+0.67[d]				
11	+0.53[d]	−5.20	−1.71	3.49	2.99
	+0.89[e]				
12	+0.27[d]	−4.91	−1.14	3.77	3.02
	+0.67[d]				
13	+0.89[e]	−5.55	−0.96	4.59	3.49
14	+0.71[d]	−5.37	−0.89	4.48	3.39

[a]All potentials are given versus the Fc^+/Fc couple used as external standard; Scan rate = 100 mV s^{-1}. [b]B3LYP/6-311G**//B3LYP/6-31G*. [c]The values are obtained from λ_{onset}. [d]Reversible wave. [e]Irreversible wave.

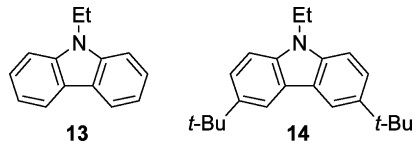

13 **14**

Most of bicarbazoles underwent two reversible or irreversible $1e^-$ oxidations, reflecting that they possess the two carbazole moieties as a redox center (Figure 4). Bicarbazoles **1**, **3**, **4**, **7**, **10**, and **12** experienced the two reversible $1e^-$ oxidation steps. On the other hand, the irreversible oxidation behavior and/or the substantial peak amplitude after the first oxidation were observed for **2**, **5**, **6**, **8**, **9**, and **11**, indicative of the instability of the radical-cationic species generated by the $1e^-$ oxidation. Compounds **1**, **4**, **7**, and **10** bearing the *t*-Bu groups underwent reversible oxidations irrespective of the π-spacers. It is well documented that the radical-cationic species of *N*-substituted carbazole derivatives easily dimerize at their 3,6-positions.[1b]

dx.doi.org/10.1021/jo3016538 | J. Org. Chem. 2012, 77, 9120−9133

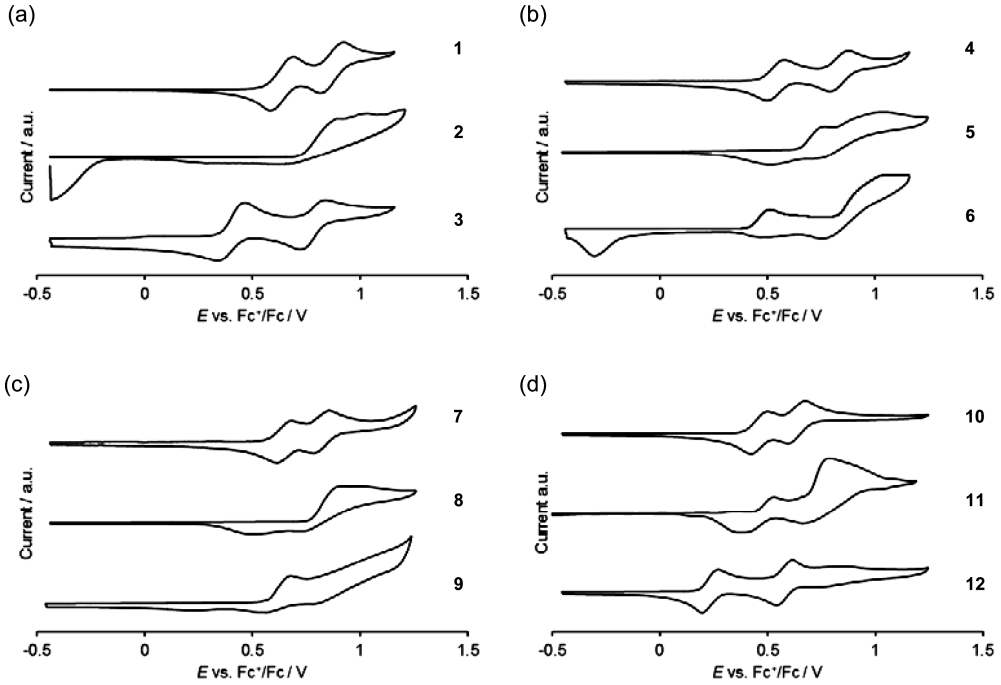

Figure 4. Cyclic voltammograms of (a) **1**–**3**, (b) **4**–**6**, (c) **7**–**9**, and (d) **10**–**12** measured in CH_2Cl_2 (0.1 mol/L n-Bu_4NPF_6) at scan rate 100 mV/s.

Thus, the *t*-Bu groups in **1**, **4**, **7**, and **10** appear to sufficiently suppress the decomposition and/or dimerization processes of the cationic species formed upon electron release. It is worth noting **3**, **6**, **9**, and **12**, where the two carbazole moieties are linked at the 3-position, differ much in the reversibility of the oxidation and back-oxidation processes. Thus, **3** and **12** are oxidized reversibly, whereas **6** and **9** are irreversibly. These results indicate that an acetylenic spacer relative to an olefinic spacer lowers the reversibility for conjugated carbazole systems. It seems that the electron-accepting ability of an acetylenic spacer as compared to an olefinic spacer decreases the kinetic stability of electronically generated cationic species.

Bicarbazole **1** showed almost the same oxidation potential as that of **14** (+0.70 V (**1**), +0.71 V (**14**)). These results clearly confirm the lack of effective π-conjugation between the two carbazole moieties in **1** and are in good agreement with those in the UV–vis spectra. The first oxidation of **2** and **3** occurs at lower oxidation potentials than that of **13** (+0.74 V (**2**), +0.46 V (**3**), +0.89 (**13**)). Thus, the direct connection of the two carbazole moieties at the 2- and 3-positions enhances the donor ability and the latter has the pronounced effect. Bicarbazoles **5** and **6** display slightly anodic shifts of the E_{pa} values as compared to those for **2** and **3**, respectively (+0.77 V (**5**), +0.51 V (**6**)), which should reflect the electron-accepting ability and the decoupling effect of the ethnylene spacer.[33] In contrast, **4** is oxidized at the lower potential than **1** by 130 mV. The difference between the first E_{pa} and the second E_{pa} for **4** is 300 mV, while that for **1** is 230 mV. These results clearly confirm that the two carbazole moieties in **4** are effectively conjugated owing to the release of twisting as revealed by X-ray analysis. The first E_{pa} values of **7**–**9** with the butadiynylene spacer are anodically shifted relative to those of the corresponding **4**–**6** (+0.68 V (**7**), +0.91 V (**8**), +0.67 V (**9**)), which is readily explained by the stronger electron-accepting ability of a butadiynylene spacer than an ethynylene spacer.[33]

Bicarbazoles **10**–**12** with the ethenylene spacer displayed remarkable cathodic shifts of the first E_{pa} values relative to **4**–**6** with the ethynylene spacer, respectively, by 80–240 mV (+0.49 V (**10**), +0.53 (**11**), +0.27 V (**12**)). Compounds **11** and **12** are easily oxidized as compared to **2** by 210 mV and **3** by 190 mV, respectively. Thus, in sharp contrast to an ethynylene spacer, an ethenylene spacer was found to enhance the donor ability of bicarbazole π-systems, although the reason for this finding is not clear at present. The similar effects of acetylenic and olefinic spacers on donor potency were seen in π-extended tetrathiafulvalene derivatives by Nielsen and co-workers.[34] As summarized in Table 2, it is worth stating that there is a clear relationship between the conjugation connectivity of the two carbazole moieties and the first E_{pa} values, and thus the trend of the 2- < 1- < 3-positions in order of lowering the first E_{pa} values is generally applicable to **1**–**12**. Consequently, **12** has the lowest first E_{pa} value. A similar trend has been also observed in our recent thienylcarbazole systems.[16]

TD-DFT and Frontier Molecular Orbital (FMO) Calculations. We performed the time-dependent (TD) DFT calculations (TD-B3LYP/6-31G*//B3LYP/6-31G*) for **1**–**12** in order to gain insight into their electronic transitions, and the results are summarized at Table 1. On the basis of the theoretical calculations, the absorption maxima in the low-energy region of **3**–**5**, **7**–**9**, **10**, and **11** are mainly attributable to the HOMO–LUMO transitions, whereas those of **1**, **2**, **6**, and **12** are related to the largely mixed transitions from HOMO, HOMO-1, and HOMO-2 to LUMO, LUMO+1, and LUMO+2. In general, the longest λ_{max} values estimated by the calculations are in good agreement with those obtained by the experiments. The calculations reproduced well the experimentally observed findings that the insertion of π-conjugated spacers between the two carbazole moieties results in the bathochromic shifts of the longest λ_{max} values and the connection at the 1-position of carbazole causes the bathochromic shift in the longest λ_{max} compared to that at the 2- and 3-positions. However, the effect of the ethenylene spacer on the longer wavelength shifts seems to be underestimated than relative to the butadiynylene spacer.

dx.doi.org/10.1021/jo3016538 | J. Org. Chem. 2012, 77, 9120–9133

We subjected **1**−**12** to the single-point calculations at the level of B3LYP/6-311G**//B3LYP/6-31G* to obtain the FMO plots and the HOMO and LUMO levels. The results are listed in Table 2, and the HOMOs and LUMOs of **1**−**12** are shown in Figure 5. The theoretically calculated HOMO−LUMO gaps ($\Delta E_{HOMO-LUMO}$) are higher than those obtained in the UV−vis spectroscopic measurements (ΔE_{opt}) by ca. 0.5 eV, probably reflecting that the calculations are employed under the gas-phase conditions. With respect to the effects of the conjugation connectivity and the π-spacers in bicarbazoles on their HOMO and LUMO levels, the theoretical calculations provide the following four important findings, which are generally consistent with the results obtained by the absorption spectra and CV. (1) In essentially planar bicarbazole π-systems, the connection at the 1-position of carbazole allows the smallest $\Delta E_{HOMO-LUMO}$ values, namely the high extent of π-conjugation, and that at the 3-position allows the largest values. Exceptionally, the HOMO−LUMO gap of **10** is estimated to be larger than that of **11** in the calculations (3.69 eV (**10**), 3.49 eV (**11**)). (2) The connection at the 3-position of carbazole ensures high HOMO levels and makes the molecules strong donors relative to that at the 1- and 2-positions. (3) The $\Delta E_{HOMO-LUMO}$ values become smaller upon introduction of the π-spacers, and an ethenylene spacer effectively decreases the $\Delta E_{HOMO-LUMO}$ values as compared to an ethynylene spacer. (4) The introduction of an ethenylene spacer sufficiently elevates the HOMO levels of the resulting bicarbazoles, and thus **10**−**12** become stronger donors than the corresponding **1**−**3**.[35]

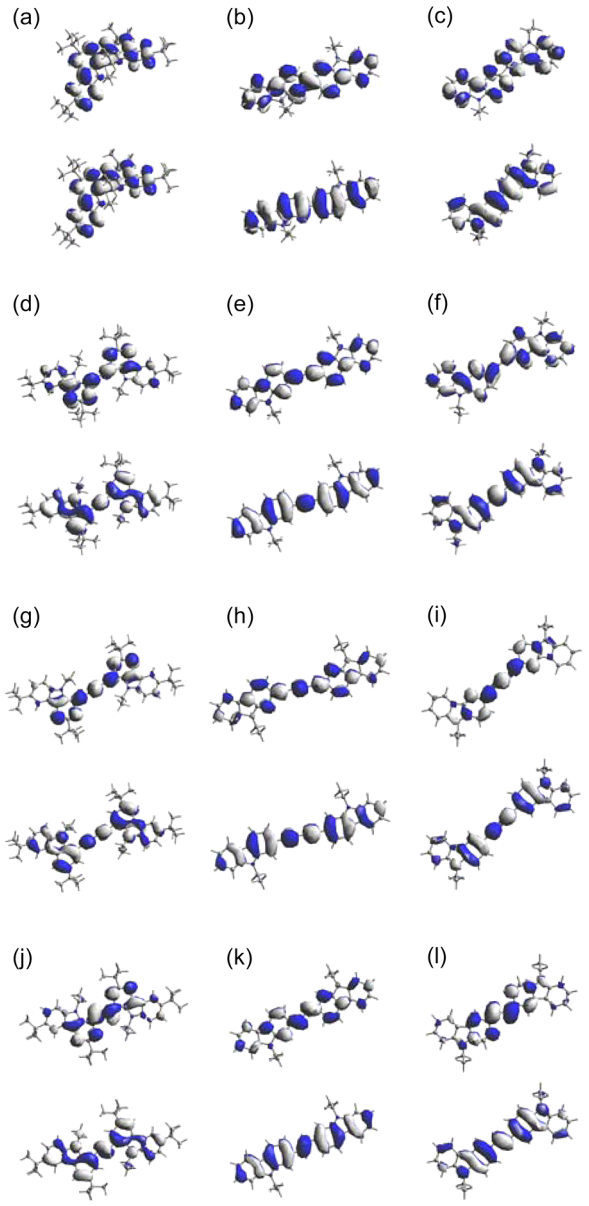

Figure 5. Molecular orbital plots (B3LYP/6-311G**//B3LYP/6-31G*) of (a) **1**, (b) **2**, (c) **3**, (d) **4**, (e) **5**, (f) **6**, (g) **7**, (h) **8**, (i) **9**, (j) **10**, (k) **11**, and (l) **12**. The lower plots represent the HOMOs, and the upper plots represent the LUMOs.

All the HOMOs of **1**−**12** are evenly delocalized over the entire molecular π-frameworks as shown in Figure 5.[36] The LUMOs of **1**−**6**, **8**, and **11** are also delocalized over the entire π-frameworks, while those of **7**, **9**, **10**, and **12** are slightly localized at the central butadiynylene or ethenylene segment.[37] It is interesting to note that the HOMO densities of **2**, **5**, **8**, and **11** have almost no contribution from the electron-rich nitrogen atoms, whereas those of other compounds are found on the nitrogen atoms. This finding explains that the connection at the 2-position of carbazole makes the molecules weak donors as compared to that at the 1- and 3-positions, however, at present we do not have a suitable explanation for the difference in effectiveness for the donor potency between the connection at the 1-position and that at the 3-position.

CONCLUSION

In conclusion, we have synthesized a series of bicarbazoles **1**−**12** by means of Suzuki−Miyaura, Sonogashira, Hay, and McMurry coupling reactions as key steps. The electronic structures were approached by UV−vis and fluorescence spectral measurements, CV, and DFT calculations as well as X-ray analyses. Based on this study, a following clear picture about the effects of the structural variations of bicarbazoles, namely the conjugation connectivity and the insertion of acetylenic and olefinic spacers, on their electronic and electrochemical properties emerges. The connection at the 1-position of carbazole results in high extent of π-conjugation of the molecules as observed in the absorption spectra of **4**, **7**, and **10**, while that at the 3-position enhances the donor ability of the molecules as confirmed by the CV for **3**, **6**, **9**, and **12**. The introduction of π-spacers steadily brings about the extension of π-conjugation, and an ethenylene spacer has a pronounced effect relative to an ethynylene spacer. The introduction of ethynylene and butadiynylene spacers decreases the donor ability owing to the electron-accepting effect of the acetylenic spacers, but on the contrary, the introduction of an ethenylene spacer increases the donor ability. The structural variations of bicarbazoles alter the fluorescence quantum yields dramatically, which vary from 0.002 to 0.84. In general, the experimentally obtained structure−property relationships are in qualitative agreement with the findings obtained by DFT calculations. We believe that the present study provides valuable information for the design and synthesis of new carbazole-based π-systems.

EXPERIMENTAL SECTION

General Sonogashira Cross-Coupling Procedure. A solution of haloarene (1 equiv) in Et_3N (~50 mmol/L) was bubbled with argon with stirring for 15 min. $PdCl_2(PPh_3)_2$ (0.03 equiv), CuI (0.25 equiv), PPh_3 (0.09 equiv), and alkyne (0.8−1.2 equiv) were added to the mixture, and the resulting mixture was bubbled for further 15 min. The mixture was heated under argon atmosphere. The solvent was

dx.doi.org/10.1021/jo3016538 | J. Org. Chem. 2012, 77, 9120−9133

removed in vacuo and the residue was dissolved in CH_2Cl_2. The resulting solution was washed with water, dried over $MgSO_4$, and evaporated in vacuo. The residue was purified by column chromatography. An analytically pure material was obtained by recycling gel permeation chromatography (GPC) eluting with $CHCl_3$.

General Hay Coupling Procedure. A mixture of ethynylcarbazole (1 equiv), CuCl (8 equiv), and *N*,*N*,*N*′,*N*′-tetramethylethylenediamine (8 equiv) in toluene (~30 mmol/L) was stirred at 50−70 °C under air supply. The suspension was filtered through a bed of silica gel, and the filtrate was removed in vacuo. The residue was purified by column chromatography. An analytically pure material was obtained by recycling gel permeation chromatography (GPC) eluting with $CHCl_3$.

Preparation of 1. A mixture of bromide **15** (0.48 g, 1.24 mmol), boronic acid ester **16** (0.30 g, 0.69 mmol), K_2CO_3 (0.40 g, 2.89 mmol), and $Pd(PPh_3)_4$ (10 mg, 8.65 μmol) in toluene (25 mL) and water (5 mL) was refluxed for 24 h under argon atmosphere. After the mixture was diluted with CH_2Cl_2 (50 mL), the resulting solution was washed with water (100 mL × 2), dried over anhydrous $MgSO_4$, and evaporated in vacuo. The residue was purified by column chromatography (SiO_2; hexane/toluene 3:1) and recycling GPC to give **1** (360 mg, 84%) as white solids. Mp 177−180 °C; ^{1}H NMR (300 MHz, $CDCl_3$): δ = 0.78 (t, J = 6.9 Hz, 6H), 1.48 (s, 18H), 1.49 (s, 18H), 3.40−3.52 (m, 2H), 3.62−3.74 (m, 2H), 7.20 (d, J = 8.7 Hz, 2H), 7.49 (dd, J = 2.1, 8.7 Hz, 2H), 7.50 (d, J = 2.1 Hz, 2H), 8.17 (d, J = 2.1 Hz, 2H), 8.19 (d, J = 2.1 Hz, 2H); ^{13}C NMR (125 MHz, $CDCl_3$): δ = 14.4, 32.18, 32.24, 34.8, 38.4, 108.1, 115.8, 116.2, 122.6, 122.9, 123.4, 123.6, 126.7, 136.9, 139.3, 141.0, 141.9 (one peak was missing); UV−vis (CH_2Cl_2): λ_{max} (relative intensity) = 269 (1.00), 301 (0.85), 342 (0.20), 356 nm (0.23); EI-MS (70 eV): m/z 612 (M^+); Elemental analysis calcd (%) for $C_{44}H_{56}N_2$·0.01$CHCl_3$: C 86.07, H 9.19, N 4.56; found C 85.80, H 9.29, N 4.59.

Preparation of 2. To a solution of bromide **17** (0.17 g, 0.63 mmol) in THF (15 mL), a hexane solution of *n*-BuLi (0.60 mL, 0.98 mmol, 1.65 mol/L) was added dropwise at −78 °C under argon atmosphere. After the mixture was stirred at room temperature for 1 h, a solution of trimethoxyborane (0.21 mL, 1.89 mmol) in THF (2 mL) was added dropwise to the mixture at −78 °C. The mixture was stirred at −78 °C for 1 h and at room temperature for 3 h, and quenched by addition of aqueous HCl (20 mL, 3 N). The organic phase was separated, and the aqueous phase was extracted with EtOAc (25 mL × 3). The combined organic phase was washed with brine (70 mL × 2), dried over anhydrous $MgSO_4$, and evaporated in vacuo. After the residue was suspended in hexane, the precipitate was collected by filtration and washed with hexane to give crude **18** (0.049 g) as white solids, which was used in the next reaction without further purification. ^{1}H NMR (300 MHz, $CDCl_3$): δ = 1.60 (t, J = 7.2 Hz, 3H), 4.58 (q, J = 7.2 Hz, 2H), 7.27−7.32 (m, 1H), 7.49−7.59 (m, 2H), 8.21−8.24 (m, 2H), 8.30 (d, J = 7.8 Hz, 1H), 8.41 (s, 1H).

A mixture of bromide **17** (0.067 g, 0.24 mmol), crude boronic acid **18** (0.049 g), K_2CO_3 (0.070 g, 0.51 mmol), and $Pd(PPh_3)_4$ (10 mg, 8.65 μmol) in toluene (7 mL) and water (1 mL) was refluxed for 24 h under argon atmosphere. After the mixture was diluted with CH_2Cl_2 (50 mL), the resulting solution was washed with water (100 mL × 2), dried over anhydrous $MgSO_4$, and evaporated in vacuo. The residue was purified by column chromatography (SiO_2; hexane/toluene 3:1) and recycling GPC to give **2** (41 mg, 17% based on **17** via **18**) as white solids. Mp 242−246 °C; ^{1}H NMR (300 MHz, $CDCl_3$): δ = 1.50 (t, J = 7.2 Hz, 6H), 4.48 (q, J = 7.2 Hz, 4H), 7.23−7.28 (m, 2H), 7.43−7.51 (m, 4H), 7.61 (dd, J = 1.2, 8.1 Hz, 2H), 7.71 (d, J = 1.2 Hz, 2H), 8.14 (dd, J = 1.5, 7.8 Hz, 2H), 8.19 (d, J = 8.1 Hz, 2H); ^{13}C NMR (125 MHz, $CDCl_3$): δ = 14.0, 37.7, 107.5, 108.6, 119.0, 119.2, 120.6, 120.7, 122.1, 122.9, 125.7, 140.3, 140.59, 140.66; UV−vis (CH_2Cl_2): λ_{max} (relative intensity) = 267 (1.00), 326 (0.66), 350 nm (sh, 0.46); EI-MS (70 eV): m/z 388 (M^+); Elemental analysis calcd (%) for $C_{28}H_{24}N_2$·0.04$CHCl_3$: C 85.63, H 6.16, N 7.12; found C 85.69, H 6.09, N 7.10.

Preparation of 4. Iodide **19** (0.06 g, 0.14 mmol) was allowed to react with ethynylcarbazole **21** (0.03 g, 0.091 mmol) at 80 °C for 20 h according to the general Sonogashira cross-coupling procedure. The crude material was purified by column chromatography (SiO_2; hexane/toluene 9:1) and recycling GPC to give **4** (23 mg, 40%) as white solids. Mp > 250 °C; ^{1}H NMR (300 MHz, $CDCl_3$): δ = 1.48 (s, 18H), 1.49 (s, 18H), 1.63 (t, J = 7.2 Hz, 6H), 4.98 (q, J = 7.2 Hz, 4H), 7.39 (d, J = 8.7 Hz, 2H), 7.57 (dd, J = 2.1, 8.7 Hz, 2H), 7.69 (d, J = 2.1 Hz, 2H), 8.12 (d, J = 2.1 Hz, 2H), 8.13 (d, J = 2.1 Hz, 2H); ^{13}C NMR (125 MHz, $CDCl_3$): δ = 15.8, 32.0, 32.2, 34.6, 34.8, 38.8, 90.5, 104.6, 108.2, 116.3, 117.4, 122.5, 124.0, 124.2, 128.1, 137.4, 139.1, 141.5, 142.2; UV−vis (CH_2Cl_2): λ_{max} (relative intensity) = 260 (sh, 0.82), 279 (0.70), 306 (1.00), 345 (sh, 0.14), 384 (0.44), 400 nm (0.52); HR-FAB-MS (NBA, positive): m/z calcd for $C_{46}H_{56}N_2^+$ 636.4443, found 636.4442 (M^+).

Preparation of 5. A mixture of **22** (0.20 g, 0.69 mmol) and K_2CO_3 (0.24 g, 1.72 mmol) in MeOH (10 mL) and THF (10 mL) was stirred at room temperature for 5 h. After the solvent was removed in vacuo, the residue was extracted with CH_2Cl_2 (50 mL). The resulting mixture was washed with water (100 mL × 2), dried over anhydrous $MgSO_4$, and evaporated in vacuo to give crude **23** (0.19 g) as yellow oil, which was used in the next reaction without further purification due to the instability. We observed the decomposition of **23** by passing through silica gel column chromatography.

A mixture of bromide **17** (0.201 g, 0.73 mmol), LiI (0.970 g, 7.25 mmol), and CuI (1.39 g, 7.30 mmol) in DMSO (40 mL) was stirred at 150 °C for 24 h. The reaction was quenched by addition of aqueous $NaHSO_3$ (50 mL, 5% w/v). The organic phase was separated, and the aqueous phase was extracted with CH_2Cl_2 (50 mL × 3). The combined organic phase was washed with brine (100 mL × 2), dried over anhydrous $MgSO_4$, and evaporated in vacuo. The residue was purified by column chromatography (SiO_2; hexane/toluene 9:1) to give crude **24** (0.210 g) as white solids, which contains *ca.* 10% of unreacted **17** as an inseparable material. The crude **24** was used in the next reaction without further purification. ^{1}H NMR (300 MHz, $CDCl_3$): δ = 1.43 (t, J = 7.2 Hz, 3H), 4.31 (q, J = 7.2 Hz, 2H), 7.23−7.28 (m, 1H), 7.40 (d, J = 7.8 Hz, 1H), 7.47−7.56 (m, 2H), 7.77 (d, J = 1.2 Hz, 1H), 7.83 (d, J = 8.1 Hz, 1H), 8.07 (d, J = 7.8 Hz, 1H).

A solution of crude iodide **24** (0.210 g) in Et_3N (15 mL) and THF (15 mL) was bubbled with argon with stirring for 15 min. $Pd(PPh_3)_4$ (0.15 g, 0.13 mmol) and crude ethynylcarbazole **23** (0.19 g) were added and the resulting mixture was bubbled for further 15 min. After the mixture was refluxed for 30 h under argon atmosphere, the solvents were removed in vacuo. After the residue was dissolved in CH_2Cl_2 (50 mL), the resulting solution was washed with water (50 mL × 2), dried over anhydrous $MgSO_4$, and evaporated in vacuo. The residue was purified by column chromatography (SiO_2; hexane/toluene 3:1), recycling GPC, and recrystallization from CH_2Cl_2/hexane to give **5** (80 mg, 30% based on **22**) as white solids. Mp 233−236 °C; ^{1}H NMR (300 MHz, $CDCl_3$): δ = 1.48 (t, J = 7.2 Hz, 6H), 4.41 (q, J = 7.2 Hz, 4H), 7.22−7.28 (m, 2H), 7.43 (d, J = 8.1 Hz, 2H), 7.45−7.52 (m, 4H), 7.67 (s, 2H), 8.08 (dd, J = 0.6, 8.1 Hz, 2H), 8.10 (d, J = 7.8 Hz, 2H); ^{13}C NMR (125 MHz, $CDCl_3$): δ = 14.0, 37.7, 90.5, 108.7, 111.8, 119.2, 120.3, 120.5, 120.7, 122.69, 122.79, 123.0, 126.2, 139.7, 140.7; UV−vis (CH_2Cl_2): λ_{max} (relative intensity) = 265 (1.00), 280 (sh, 0.38), 320 (sh, 0.63), 343 (0.95), 369 nm (0.91); HR-FAB-MS (NBA, positive): m/z calcd for $C_{30}H_{24}N_2^+$ 412.1939, found 412.1934 (M^+).

Preparation of 6. Iodide **25** (0.26 g, 0.81 mmol) was allowed to react with ethynylcarbazole **27** (0.12 g, 0.55 mmol) at 80 °C for 16 h according to the general Sonogashira cross-coupling procedure. The crude material was purified by column chromatography (SiO_2; hexane/toluene 3:1) and recycling GPC to give **6** (80 mg, 35%) as white solids. Mp 226−230 °C; ^{1}H NMR (500 MHz, $CDCl_3$): δ = 1.46 (t, J = 7.2 Hz, 6H), 4.38 (q, J = 7.2 Hz, 4H), 7.26−7.29 (m, 2H), 7.39 (d, J = 8.4 Hz, 2H), 7.42 (d, J = 8.4 Hz, 2H), 7.49−7.52 (m, 2H), 7.70 (dd, J = 1.5, 8.4 Hz, 2H), 8.13 (dd, J = 0.9, 7.8 Hz, 2H), 8.36 (d, J = 1.5 Hz, 2H); ^{13}C NMR (125 MHz, $CDCl_3$): δ = 13.9, 37.7, 88.8, 108.6, 108.7, 113.9, 119.3, 120.7, 122.7, 123.0, 124.0, 126.1, 129.3, 139.4, 140.4; UV−vis (CH_2Cl_2): λ_{max} (relative intensity) = 276 (0.51), 305 (1.00), 323 (0.77), 340 (sh, 0.53), 350 (sh, 0.38), 365 nm (sh, 0.15); HR-FAB-MS (NBA, positive): m/z calcd for $C_{30}H_{24}N_2^+$ 412.1939, found 412.1937 (M^+).

dx.doi.org/10.1021/jo3016538 | J. Org. Chem. 2012, 77, 9120−9133

Preparation of 7. Ethynylcarbazole **21** (100 mg, 0.302 mmol) was allowed to react at 50 °C for 24 h according to the general Hay coupling procedure. The crude material was purified by column chromatography (SiO_2; hexane/toluene 1:1) and recycling GPC to give **7** (74 mg, 74%) as yellow solids. Mp >250 °C; ^{1}H NMR (300 MHz, $CDCl_3$): δ = 1.46 (s, 36H), 1.55 (t, J = 7.2 Hz, 6H), 4.83 (q, J = 7.2 Hz, 4H), 7.37 (d, J = 8.4 Hz, 2H), 7.56 (d, J = 8.4 Hz, 2H), 7.71 (s, 2H), 8.09 (s, 2H), 8.14 (s, 2H); ^{13}C NMR (125 MHz, $CDCl_3$): δ = 15.5, 32.0, 32.1, 34.7, 34.8, 38.8, 81.2, 102.5, 108.3, 116.3, 118.6, 122.4, 124.21, 124.31, 130.0, 138.4, 139.1, 141.6, 142.4 (1 peek was missing); UV−vis (CH_2Cl_2): λ_{max} (relative intensity) = 290 (sh, 0.79), 303 (1.00), 330 (sh, 0.34), 394 (0.69), 412 nm (0.70); MALDI-TOF-MS (Dith, positive): m/z 661.39 ([M + H]$^+$); Elemental analysis calcd (%) for $C_{48}H_{36}N_2$·0.14$CHCl_3$: C 85.32, H 8.35, N 4.13, found: C 85.36, H 8.39, N 4.14.

Preparation of 8. A mixture of **22** (0.27 g, 0.92 mmol) and K_2CO_3 (0.32 g, 2.31 mmol) in MeOH (10 mL) and THF (10 mL) was stirred at room temperature for 5 h. After the solvent was removed in vacuo, the residue was extracted with CH_2Cl_2 (50 mL). The resulting mixture was washed with water (100 mL × 2), dried over anhydrous $MgSO_4$, and evaporated in vacuo to give crude **23** (0.20 g) as yellow oil, which was used in the next reaction without further purification due to the instability.

The crude ethynylcarbazole **23** (0.20 g) was allowed to react at 50 °C for 24 h according to the general Hay coupling procedure. The crude material was purified by column chromatography (SiO_2; hexane/toluene 1:1) and recycling GPC to give **8** (74 mg, 37% based on **22**) as yellow solids. Mp 194−196 °C; ^{1}H NMR (300 MHz, $CDCl_3$): δ = 1.45 (t, J = 7.2 Hz, 6H), 4.37 (q, J = 7.2 Hz, 4H), 7.26 (t, J = 7.2 Hz, 2H), 7.43 (d, J = 8.1 Hz, 4H), 7.51 (t, J = 8.1 Hz, 2H), 7.64 (s, 2H), 8.06 (d, J = 9.0 Hz, 2H), 8.09 (d, J = 7.8 Hz, 2H); ^{13}C NMR (125 MHz, $CDCl_3$): δ = 13.9, 37.6, 73.9, 83.3, 108.7, 112.8, 118.4, 119.4, 120.5, 120.9, 122.5, 123.3, 123.8, 126.6, 139.3, 140.8; UV−vis (CH_2Cl_2): λ_{max} (relative intensity) = 264 (1.00), 305 (sh, 0.23), 340 (sh, 0.74), 354 (0.84), 382 nm (0.73); MALDI-TOF-MS (Dith, positive): m/z 437.09 ([M + H]$^+$); Elemental analysis calcd (%) for $C_{32}H_{24}N_2$·0.06$CHCl_3$: C 86.78, H 5.47, N 6.31, found: C 86.70, H 5.28, N 6.12.

Preparation of 9. Ethynylcarbazole **27** (41 mg, 0.186 mmol) was allowed to react at 70 °C for 24 h according to the general Hay coupling procedure. The crude material was purified by column chromatography (SiO_2; hexane/toluene 1:1) and recycling GPC to give **9** (28 mg, 68%) as yellow solids. Mp 221−224 °C; ^{1}H NMR (300 MHz, $CDCl_3$): δ = 1.45 (t, J = 7.2 Hz, 6H), 4.38 (q, J = 7.2 Hz, 4H), 7.27−7.30 (m, 2H), 7.36 (d, J = 8.4 Hz, 2H), 7.43 (d, J = 8.4 Hz, 2H), 7.48−7.51 (m, 2H), 7.65 (dd, J = 1.5, 8.4 Hz, 2H), 8.10 (d, J = 7.8 Hz, 2H), 8.32 (s, 2H); ^{13}C NMR (125 MHz, $CDCl_3$): δ = 13.9, 37.8, 72.8, 82.7, 108.7, 108.8, 119.6, 111.9, 120.7, 122.5, 123.0, 125.3, 126.4, 130.1, 140.01, 140.05; UV−vis (CH_2Cl_2): λ_{max} (relative intensity) = 280 (sh, 0.70), 299 (1.00), 342 (0.92), 360 (0.67), 372 nm (0.73); MALDI-TOF-MS (Dith, positive): m/z 437.01 ([M + H]$^+$); Elemental analysis calcd (%) for $C_{32}H_{24}N_2$·0.03$CHCl_3$: C 87.40, H 5.50, N 6.36, found: C 87.34, H 5.58, N 6.27.

Preparation of 10. To a solution of aldehyde **28** (0.102 g, 0.304 mmol) in THF (20 mL), zinc powder (0.066 g, 1.00 mmol) was added. Titanium(IV) chloride (0.050 mL, 0.456 mmol) was added dropwise to the mixture at 0 °C. After the mixture was refluxed for 4 h under argon atmosphere, the solution was added to ice water and extracted with CH_2Cl_2 (100 mL × 2). The combined organic phase was washed with brine (100 mL × 2), dried over anhydrous $MgSO_4$, and evaporated in vacuo. The residue was purified by column chromatography (SiO_2; hexane/CH_2Cl_2 9:1) to give **10** (76 mg, 78%) as yellow solids. Mp >250 °C; ^{1}H NMR (500 MHz, $CDCl_3$): δ = 1.52 (s, 18H), 1.57 (s, 18H), 1.61 (t, J = 7.2 Hz, 6H), 4.65 (q, J = 7.2 Hz, 4H). 7.38 (d, J = 8.7 Hz, 2H), 7.59 (dd, J = 1.8, 8.7 Hz, 2H), 7.73 (d, J = 1.8 Hz, 2H), 7.81 (s, 2H), 8.14 (d, J = 1.8 Hz, 2H), 8.16 (d, J = 1.8 Hz, 2H); ^{13}C NMR (125 MHz, $CDCl_3$): δ = 15.5, 32.19, 32.21, 34.79, 34.82, 40.2, 108.2, 116.1, 116.3, 122.1, 122.9, 123.0, 123.7, 124.3, 128.8, 136.4, 139.6, 141.9, 142.1; UV−vis (CH_2Cl_2): λ_{max} (relative intensity) = 270 (sh, 0.61), 303 (1.00), 378 nm (0.33); MALDI-TOF-MS (Dith, positive): m/z 639.29 ([M + H]$^+$); Elemental analysis calcd (%) for $C_{46}H_{58}N_2$·0.06$CHCl_3$: C 85.62, H 9.06 N 4.33; found C 85.44, H 9.22, N 4.37.

Preparation of 11. Zinc powder (0.110 g, 1.56 mmol) was suspended in THF (30 mL) under argon atmosphere. A solution of titanium(IV) chloride (0.30 mL, 2.60 mmol) in CH_2Cl_2 (5 mL) was added to the suspension, and then the resulting suspension was heated to reflux at 80 °C for 1 h. A solution of **29** (0.122 g, 0.52 mmol) in pyridine (2 mL) and THF (10 mL) was added dropwise to the reaction mixture. After the mixture was refluxed for 18 h, the mixture was poured into saturated aqueous $NaHCO_3$ (50 mL) and the resulting mixture was extracted with CH_2Cl_2 (100 mL × 2). The combined organic phase was washed with water (100 mL × 2), dried over anhydrous $MgSO_4$, and evaporated in vacuo. The residue was purified by column chromatography (SiO_2; hexane/CH_2Cl_2 4:1) and washed with EtOH to give **11** (12 mg, 10%) as yellow solids. Mp 198 °C (decomp.); ^{1}H NMR (400 MHz, $CDCl_3$): δ = 1.50 (t, J = 7.2 Hz, 6H), 4.43 (q, J = 7.2 Hz, 4H). 7.23 (t, J = 6.9 Hz, 2H), 7.40−7.48 (m, 4H), 7.46 (s, 2H), 7.51 (d, J = 8.0 Hz, 2H), 7.58 (s, 2H), 8.09 (d, J = 8.0 Hz, 4H); ^{13}C NMR (150 MHz, $CDCl_3$): δ = 14.1, 37.7, 106.6, 108.6, 117.9, 119.1, 120.5, 120.7, 122.7, 123.0, 125.7, 129.3, 135.5, 140.6, 140.7; UV−vis (CH_2Cl_2): λ_{max} (relative intensity) = 267 (0.68), 285 (sh, 0.28), 368 (1.00), 385 nm (sh, 0.79). HR-FAB-MS (NBA, positive): m/z calcd for $C_{30}H_{26}N_2^+$ 414.2096, found 414.2095 (M$^+$).

Preparation of 15. To a solution of **14** (3.08 g, 0.010 mol) in DMF (100 mL), *N*-bromosuccinimide (1.78 g, 0.010 mol) was added and the mixture was stirred at room temperature for 3 h under light protection. Water (100 mL) was added and the resulting mixture was extracted with CH_2Cl_2 (50 mL × 3). The combined organic phase was washed with water (150 mL × 2), dried over anhydrous $MgSO_4$, and evaporated in vacuo. The residue was purified by column chromatography (SiO_2; hexane) to give **15** (3.45 g, 90%) as white solids. Mp 112−115 °C; ^{1}H NMR (300 MHz, $CDCl_3$): δ = 1.43 (t, J = 7.2 Hz, 3H) 1.43−1.45 (m, 18H), 4.76 (q, J = 7.2 Hz, 2H), 7.34 (d, J = 8.7 Hz, 1H), 7.55 (dd, J = 1.8, 8.7 Hz, 1H), 7.60 (d, J = 1.8 Hz, 1H), 8.02 (d, J = 1.8 Hz, 1H), 8.05 (d, J = 1.8 Hz, 1H); ^{13}C NMR (125 MHz, $CDCl_3$): δ = 15.7, 32.0, 32.1, 34.6, 34.8, 38.7, 102.4, 108.5, 115.6, 116.1, 122.3, 124.3, 126.3, 128.7, 135.0, 139.6, 142.4, 143.2; UV−vis (CH_2Cl_2): λ_{max} (relative intensity) = 255 (1.00), 270 (0.74), 290 (sh, 0.40), 298 (0.63), 325 (sh, 0.07), 341 (0.14), 355 nm (0.15); HR-FAB-MS (NBA, positive): m/z calcd for $C_{22}H_{28}BrN^+$ 385.1405, found 385.1403 (M$^+$).

Preparation of 16. To a solution of bromide **15** (1.56 g, 4.04 mmol) in Et_2O (80 mL), a hexane solution of *n*-BuLi (3.00 mL, 4.95 mmol, 1.65 mol/L) was added dropwise at −78 °C under argon atmosphere. After the mixture was stirred at room temperature for 1 h, 2-isopropoxy-4,4,5,5-tetramethyl-1,3,2-dioxaborolane (2.00 mL, 9.89 mmol) was added dropwise to the mixture at −78 °C. The mixture was stirred at room temperature for 3 h and the resulting mixture was poured into aqueous NH_4Cl (100 mL, 5% w/v). The organic phase was separated, and the aqueous phase was extracted with EtOAc (50 mL × 3). The combined organic phase was washed with brine (100 mL × 2), dried over anhydrous $MgSO_4$, and evaporated in vacuo. The residue was purified by column chromatography (SiO_2; hexane/toluene 1:1) to give **16** (1.00 g, 57%) as white solids. Mp 198−201 °C; ^{1}H NMR (300 MHz, $CDCl_3$): δ = 1.38 (t, J = 7.2 Hz, 3H), 1.44 (s, 12H), 1.46 (s, 18H), 4.65 (q, J = 7.2 Hz, 2H), 7.34 (d, J = 8.7 Hz, 1H), 7.51 (dd, J = 1.5, 8.7 Hz, 1H), 7.90 (d, J = 2.1 Hz, 1H), 8.09 (d, J = 1.5 Hz, 1H), 8.21 (d, J = 2.1 Hz, 1H); ^{13}C NMR (125 MHz, $CDCl_3$): δ = 14.4, 24.9, 32.14, 32.22, 34.6, 34.7, 39.0, 84.0, 108.3, 115.9, 119.6, 122.9, 123.3, 131.6, 139.3, 140.4, 141.6, 142.0 (two peaks were missing); UV−vis (CH_2Cl_2): λ_{max} (relative intensity) = 282 (1.00), 303 (0.61), 348 (0.19), 360 nm (0.21); MALDI-TOF-MS (Dith, positive): m/z 434.21 ([M + H]$^+$); Elemental analysis calcd (%) for $C_{28}H_{40}BNO_2$: C 77.59, H 9.30 N 3.23; found C 77.29, H 9.42, N 3.24.

Preparation of 19. To a solution of **14** (2.00 g, 6.50 mmol) in EtOH (20 mL) was added dropwise a solution of ICl (0.65 mL, 13.0 mmol) in EtOH at 78 °C. After the mixture was refluxed for 10 h, the solvent was removed in vacuo, and the residue was dissolved in CH_2Cl_2 (50 mL). The resulting solution was washed with aqueous

dx.doi.org/10.1021/jo3016538 | J. Org. Chem. 2012, 77, 9120−9133

$NaHSO_3$ (200 mL), dried over anhydrous $MgSO_4$, and evaporated in vacuo. The residue was purified by column chromatography (SiO_2; hexane/toluene 9:1) to give **19** (1.07 g, 38%) as white solids. Mp 115−118 °C; ^{1}H NMR (300 MHz, $CDCl_3$): δ = 1.42 (t, J = 7.2 Hz, 3H), 1.42 (s, 9H), 1.45 (s, 9H), 4.76 (q, J = 7.2 Hz, 2H), 7.35 (d, J = 8.7 Hz, 1H), 7.54 (dd, J = 2.1, 8.7 Hz, 1H), 7.91 (d, J = 1.8 Hz, 1H), 8.05 (d, J = 2.1 Hz, 1H), 8.06 (d, J = 1.8 Hz, 1H); ^{13}C NMR (125 MHz, $CDCl_3$): δ = 15.7, 32.0, 32.1, 34.4, 34.8, 38.0, 72.0, 108.6, 115.9, 116.5, 122.0, 124.3, 125.8, 136.1, 137.6, 139.8, 142.5, 143.6; UV−vis (CH_2Cl_2): λ_{max} (relative intensity) = 255 (1.00), 270 (0.89), 290 (sh, 0.44), 299 (0.65), 325 (sh, 0.08), 343 (0.15), 357 nm (0.17); HR-FAB-MS (NBA, positive): m/z calcd for $C_{22}H_{28}IN^+$ 433.1266, found 433.1259 (M^+).

Preparation of 20. Iodide **19** (0.52 g, 1.20 mmol) was allowed to react with 2-methyl-3-butyn-2-ol (0.50 mL, 5.11 mmol) at 60 °C for 8 h according to the general Sonogashira cross-coupling procedure. The crude material was purified by column chromatography (SiO_2; hexane/toluene 3:1) to give **20** (0.323 g, 69%) as yellow solids. Mp 202−205 °C; ^{1}H NMR (300 MHz, $CDCl_3$): δ = 1.44 (s, 9H), 1.46 (s, 9H), 1.48 (t, J = 7.2 Hz, 3H), 1.71 (s, 6H), 2.08 (s, 1H), 4.79 (q, J = 7.2 Hz, 2H), 7.34 (d, J = 8.7 Hz, 1H), 7.54 (dd, J = 2.1, 8.7 Hz, 1H), 7.54 (d, J = 2.1 Hz, 1H), 8.07 (d, J = 2.1 Hz, 2H); ^{13}C NMR (125 MHz, $CDCl_3$): δ = 15.7, 31.5, 32.0, 32.1, 34.5, 34.7, 38.4, 65.9, 81.0, 95.8, 103.4, 108.1, 116.2, 117.5, 122.3, 123.9, 124.0, 129.0, 137.4, 139.0, 141.3, 142.1; UV−vis (CH_2Cl_2): λ_{max} (relative intensity) = 260 (0.72), 287 (1.00), 308 (0.42), 355 (0.20), 369 nm (0.28); HR-FAB-MS (NBA, positive): m/z calcd for $C_{27}H_{35}NO^+$ 389.2719, found 389.2718 (M^+).

Preparation of 21. A mixture of **20** (0.49 g, 1.26 mmol) and KOH (0.55 g, 9.80 mmol) in 2-propanol (55 mL) was refluxed for 17 h. After the solvent was removed in vacuo, the residue was extracted with CH_2Cl_2 (50 mL). The resulting mixture was successively washed with water (100 mL × 2) and brine (100 mL × 2), dried over anhydrous $MgSO_4$, and evaporated in vacuo. The residue was purified by GPC to give **21** (238 mg, 57%) as pale yellow solids. Because of the instability, **21** was used in the next reaction immediately without characterization by mass spectroscopy and elemental analysis. Mp 142−146 °C; ^{1}H NMR (300 MHz, $CDCl_3$): δ = 1.44−1.46 (m, 21H), 3.36 (s, 1H), 4.80 (q, J = 7.2 Hz, 2H), 7.34 (d, J = 8.7 Hz, 1H), 7.55 (dd, J = 1.8, 8.7 Hz, 1H), 7.64 (d, J = 1.8 Hz, 1H), 8.08 (d, J = 1.8 Hz, 1H), 8.11 (d, J = 1.8 Hz, 1H); ^{13}C NMR (125 MHz, $CDCl_3$): δ = 15.6, 32.0, 32.1, 34.6, 34.8, 38.4, 79.9, 82.6, 102.9, 108.2, 116.2, 118.0, 122.4, 124.0, 124.2, 129.8, 137.7, 139.1, 141.3, 142.2; UV−vis (CH_2Cl_2): λ_{max} (relative intensity) = 259 (0.78), 286 (1.00), 308 (0.45), 354 (0.20), 369 nm (0.27).

Preparation of 22. Bromide **17** (0.740 g, 2.70 mmol) was allowed to react with trimethylsilylacetylene (1.20 mL, 8.67 mmol) at 100 °C for 24 h according to the slightly modified general Sonogashira cross-coupling procedure; piperidine was used as a solvent. The crude material was purified by column chromatography (SiO_2; hexane/toluene 9:1) to give **22** (243 mg, 31%) as white solids. Mp 127−130 °C; ^{1}H NMR (300 MHz, $CDCl_3$): δ = 0.31 (s, 12H), 1.44 (t, J = 7.2 Hz, 3H), 4.36 (q, J = 7.2 Hz, 2H), 7.21−7.26 (m, 1H), 7.35 (d, J = 7.8 Hz, 1H), 7.40 (d, J = 8.4 Hz, 1H), 7.45−7.51 (m, 1H), 7.55 (s, 1H), 8.01 (d, J = 8.1 Hz, 1H), 8.07 (d, J = 8.1 Hz, 1H); ^{13}C NMR (75 MHz, $CDCl_3$): δ = 14.5, 31.8, 32.0, 34.5, 34.7, 41.4, 109.0, 116.0, 121.0, 122.4, 123.2, 124.4, 126.1, 130.0, 136.8, 139.7, 141.0, 142.9, 191.0; UV−vis (CH_2Cl_2): λ_{max} (relative intensity) = 261 (0.78), 271 (1.00), 315 (0.38), 351 (0.18) 367 nm (0.20); MALDI-TOF-MS (Dith, positive): m/z 291.01 (M^+); Elemental analysis calcd (%) for $C_{19}H_{21}NSi\cdot0.08CHCl_3$: C 76.13, H 7.06 N 4.65; found C 75.95, H 7.40, N 4.62.

Preparation of 26. Iodide **25** (0.85 g, 2.65 mmol) was allowed to react with 2-methyl-3-butyn-2-ol (1.00 mL, 10.2 mmol) at 60 °C for 18 h according to the slightly modified general Sonogashira cross-coupling procedure; PPh_3 was not used. The crude material was purified by column chromatography (SiO_2; hexane/toluene 3:1) to give **26** (0.71 g, 96%) as pale yellow oil. ^{1}H NMR (300 MHz, $CDCl_3$): δ = 1.44 (t, J = 7.2 Hz, 3H), 1.68 (s, 6 H), 2.07 (s, 1H), 4.36 (q, J = 7.2 Hz, 2H), 7.22−7.27 (m, 1H), 7.33 (d, J = 8.4 Hz, 1H), 7.41 (d, J = 7.8 Hz, 1H), 7.46−7.54 (m, 2H), 8.07 (dd, J = 0.6, 7.8 Hz, 1H), 8.19 (d, J = 0.6 Hz, 1H); ^{13}C NMR (125 MHz, $CDCl_3$): δ = 13.8, 31.7, 37.6, 65.8, 83.4, 91.9, 108.4, 108.7, 112.6, 119.3, 120.5, 122.5, 122.8, 124.1, 126.1, 129.3, 139.5, 140.3; UV−vis (CH_2Cl_2): λ_{max} (relative intensity) = 280 (1.00), 293 (sh, 0.43), 325 (sh, 0.04), 340 (0.06), 356 nm (0.06); HR-FAB-MS (NBA, positive): m/z calcd for $C_{19}H_{19}NO^+$ 277.1467, found 277.1473 (M^+). Compound **26** was allowed to react with KOH in 2-propanol to give **27**, the ^{1}H NMR data of which were in agreement with those reported in the literature.[38]

Preparation of 28. To a solution of bromide **15** (0.399 g, 1.03 mmol) in THF (50 mL), a hexane solution of *n*-BuLi (1.40 mL, 2.31 mmol, 1.65 mol/L) was added dropwise at −78 °C under argon atmosphere. After the mixture was stirred for 1 h, piperidine-1-carbaldehyde (0.50 mL, 4.51 mmol) was added dropwise to the mixture at −78 °C. The mixture was stirred at room temperature for 3 h, and the resulting mixture was poured into aqueous NH_4Cl (100 mL, 5% w/v). The organic phase was separated, and the aqueous phase was extracted with EtOAc (50 mL × 3). The combined organic phase was washed with brine (100 mL × 2), dried over anhydrous $MgSO_4$, and evaporated in vacuo. The residue was purified by column chromatography (SiO_2; hexane/CH_2Cl_2 7:3) to give **28** (0.244 g, 70%) as yellow solids. Mp 138−141 °C; ^{1}H NMR (500 MHz, $CDCl_3$): δ = 1.49 (t, J = 7.2 Hz, 3H), 1.60 (s, 9H), 1.62 (s, 9H), 4.80 (q, J = 7.2 Hz, 2H). 7.43 (d, J = 8.7 Hz, 1H), 7.66 (d, J = 8.7 Hz, 1H), 8.10 (s, 1H), 8.28 (s, 1H), 8.53 (s, 1H), 10.4 (s, 1H); ^{13}C NMR (125 MHz, $CDCl_3$): δ = 14.5, 31.8, 32.0, 34.5, 34.7, 41.4, 109.0, 116.0, 121.0, 122.4, 123.2, 124.4, 126.1, 130.0, 136.8, 139.7, 141.0, 142.9, 191.0; UV−vis (CH_2Cl_2): λ_{max} (relative intensity) = 260 (sh, 0.59), 271 (0.54), 303 (1.00), 335 (sh, 0.17) 392 nm (0.40); MALDI-TOF-MS (Dith, positive): m/z 336.01 ($[M + H]^+$); Elemental analysis calcd (%) for $C_{23}H_{29}NO$: C 82.34, H 8.71 N 4.18; found C 82.07, H 8.81, N 4.20.

■ ASSOCIATED CONTENT

Ⓢ Supporting Information

General experimental methods, X-ray data including cif files, theoretical data, and ^{1}H and ^{13}C NMR spectra of all new compounds. This material is available free of charge via the Internet at http://pubs.acs.org.

■ AUTHOR INFORMATION

Corresponding Author

*E-mail: nakamura@gunma-u.ac.jp. Tel: +81 277 30 1310. Fax: +81 277 30 1314.

Notes

The authors declare no competing financial interest.

■ ACKNOWLEDGMENTS

This work was supported by a Grant-in-Aid for Scientific Research from the Ministry of Education, Culture, Sports, Science and Technology, Japan, and partially performed under the Cooperative Research Program of "Network Joint Research Center for Materials and Devices" (Kyushu University). We thank Prof. Dr. Soichiro Kyushin (Gunma University) for generous permission to use an X-ray diffractometer and Prof. Dr. Teruo Shinmyozu (Kyushu University) for mass spectrometry measurements.

■ REFERENCES

(1) For recent reviews, see: (a) Grazulevicius, J. V.; Strohriegl, P.; Pielichowski, J.; Pielichowski, K. *Prog. Polym. Sci.* **2003**, *28*, 1297. (b) Morin, J.-F.; Leclerc, M.; Adès, D.; Siove, A. *Macromol. Rapid Commun.* **2005**, *26*, 761. (c) Blouin, N.; Leclerc, M. *Acc. Chem. Res.* **2008**, *41*, 1110. (d) Boudreault, P.-L. T.; Morin, J.-F.; Leclerc, M. In *Design and Synthesis of Conjugated Polymers*; Leclerc, M., Morin, J.-F., Eds.; Wiley-VCH: Weinheim, 2010; p 205.

(2) For selected examples of light-emitting materials, see: (a) Morin, J.-F.; Bourdreault, P.; Leclerc, M. *Macromol. Rapid Commun.* **2002**, *23*, 1032. (b) Liu, Y.; Nishiura, M.; Wang, Y.; Hou, Z. *J. Am. Chem. Soc.* **2006**, *128*, 5592. (c) Adhikari, R. M.; Mondal, R.; Shah, B. K.; Neckers, D. C. *J. Org. Chem.* **2007**, *72*, 4727. (d) Zhao, Z.; Zhao, Y.; Lu, P.; Tian, W. *J. Phys. Chem. C* **2007**, *111*, 6883. (e) Zhao, Z.; Xu, X.; Wang, H.; Lu, P.; Yu, G.; Liu, Y. *J. Org. Chem.* **2008**, *73*, 594. (f) Zhao, Z.; Li, J.-H.; Chen, X.; Wang, X.; Lu, P.; Yang, Y. *J. Org. Chem.* **2009**, *74*, 383. (g) Wang, H.-Y.; Liu, F.; Xie, L.-H.; Tang, C.; Peng, B.; Huang, W.; Wei, W. *J. Phys. Chem. C* **2011**, *115*, 6961. (h) Kim, S. H.; Cho, I.; Sim, M. K.; Park, S.; Park, S. Y. *J. Mater. Chem.* **2011**, *21*, 9139. (i) Yao, L.; Xue, S.; Wang, Q.; Dong, W.; Yang, W.; Wu, H.; Zhang, M.; Yang, B.; Ma, Y. *Chem.—Eur. J.* **2012**, *18*, 2707.

(3) For selected examples of host materials for emitters, see: (a) Brunner, K.; van Dijken, A.; Börner, H.; Bastiaansen, J. J. A. M.; Kiggen, N. M. M.; Langeveld, B. M. W. *J. Am. Chem. Soc.* **2004**, *126*, 6035. (b) van Dijken, A.; Bastiaansen, J. J. A. M.; Kiggen, N. M. M.; Langeveld, B. M. W.; Rothe, C.; Monkman, A.; Bach, I.; Stössel, P.; Brunner, K. *J. Am. Chem. Soc.* **2004**, *126*, 7718. (c) Tsai, M.-H.; Lin, H.-W.; Su, H.-C.; Ke, T.-H.; Wu, C.-c.; Fang, F.-C.; Liao, Y.-L.; Wong, K.-T.; Wu, C.-I. *Adv. Mater.* **2006**, *18*, 1216. (d) Tao, Y.; Wang, Q.; Yang, C.; Wang, Q.; Zhang, Z.; Zou, T.; Qin, J.; Ma, D. *Angew. Chem., Int. Ed.* **2008**, *47*, 8104. (e) Kim, S. H.; Cho, I.; Sim, M. K.; Park, S.; Park, S. Y. *J. Mater. Chem.* **2011**, *21*, 9139. (f) Chen, Y.-M.; Hung, W.-Y.; You, H.-W.; Chaskar, A.; Ting, H.-C.; Chen, H.-F.; Wong, K.-T.; Liu, Y.-H. *J. Mater. Chem.* **2011**, *21*, 14971. (g) Jeong, S. H.; Seo, C. W.; Lee, J. Y.; Cho, N. S.; Kim, J. K.; Yang, J. H. *Chem.—Asian J.* **2011**, *6*, 2895. (h) Ku, S.-Y.; Hung, W.-Y.; Chen, C.-W.; Yang, S.-W.; Mondal, E.; Chi, Y.; Wong, K.-T. *Chem.—Asian J.* **2012**, *7*, 133. (i) Zheng, C.-J.; Ye, J.; Lo, M.-F.; Fung, M.-K.; Ou, X.-M.; Zhang, X.-H.; Lee, C.-S. *Chem. Mater.* **2012**, *24*, 643.

(4) (a) Drolet, N.; Morin, J.-F.; Leclerc, N.; Wakim, S.; Tao, Y.; Leclerc, M. *Adv. Funct. Mater.* **2005**, *15*, 1671. (b) Sonntag, M.; Kreger, K.; Hanft, D.; Strohriegl, P. *Chem. Mater.* **2005**, *17*, 3031. (c) Wakim, S.; Blounin, N.; Gingras, E.; Tao, Y.; Leclerc, M. *Macromol. Rapid Commun.* **2007**, *28*, 1798. (d) Song, Y.; Di, C.-a.; Wei, Z.; Zhao, T.; Xu, W.; Liu, Y.; Zhang, D.; Zhu, D. *Chem.—Eur. J* **2008**, *14*, 4731. (e) Li, Z.; Liu, Y.; Yu, G.; Wen, Y.; Guo, Y.; Ji, L.; Qin, J.; Li, Z. *Adv. Funct. Mater.* **2009**, *19*, 2677. (f) Cho, S.; Seo, J. H.; Park, S. H.; Beaupré, S.; Leclerc, M.; Heeger, A. J. *Adv. Mater.* **2010**, *22*, 1253.

(5) For a review on carbazole derivatives for photovoltaic devices, see: (a) Beaupré, S.; Boudreault, P.-L. T.; Leclerc, M. *Adv. Mater.* **2010**, *22*, E6—E27. See also: (b) Blounin, N.; Michaud, D.; Gendron, D.; Wakim, S.; Blair, E.; Neagu-Plesu, R.; Belletête, M.; Durocher, G.; Tao, Y.; Leclerc, M. *J. Am. Chem. Soc.* **2008**, *130*, 732. (c) Blounin, N.; Michaud, A.; Leclerc, M. *Adv. Mater.* **2007**, *19*, 2295. (d) Peng, B.; Najari, A.; Liu, B.; Berrouard, P.; Gendron, D.; He, Y.; Zhou, K.; Leclerc, M.; Zou, Y. *Macromol. Chem. Phys.* **2010**, *211*, 2026.

(6) (a) Zhang, Z.-B.; Fujiki, M.; Tang, H.-Z.; Motonaga, M.; Torimitsu, K. *Macromolecules* **2002**, *35*, 1988. (b) Zhang, Z.-B.; Motonaga, M.; Fujiki, M.; McKenna, C. E. *Macromolecules* **2003**, *36*, 6956.

(7) (a) Morin, J.-F.; Leclerc, M. *Macromolecules* **2001**, *34*, 4680. (b) Dierschke, F.; Grimsdale, A. C.; Müllen, K. *Synthesis* **2003**, 2470.

(8) (a) Moser, M.; Wucher, B.; Kunz, D.; Rominger, F. *Organometallics* **2007**, *26*, 1024. (b) Mudadu, M. S.; Singh, A. N.; Thummel, R. P. *J. Org. Chem.* **2008**, *73*, 6513. (c) Barbe, J.-M.; Habermeyer, B.; Khoury, T.; Gros, C. P.; Richard, P.; Chen, P.; Kadish, K. M. *Inorg. Chem.* **2010**, *49*, 8929.

(9) (a) Hassan, L. A.; Norouzi-Arasi, H.; Wagner, M.; Enkelmann, V.; Müllen, K. *Chem. Commun.* **2011**, *47*, 970. (b) Maeda, C.; Yoneda, T.; Aratani, N.; Yoon, M.-C.; Lim, J. M.; Kim, D.; Yoshioka, N.; Osuka, A. *Angew. Chem., Int. Ed.* **2011**, *50*, 5691. (c) Maeda, C.; Yoshioka, N. *Org. Lett.* **2012**, *14*, 2122.

(10) (a) Michinobu, T.; Osako, H.; Shigehara, K. *Macromol. Rapid Commun.* **2008**, *29*, 111. (b) Michinobu, T.; Osako, H.; Shigehara, K. *Macromolecules* **2009**, *42*, 8172. (c) Michinobu, T.; Osako, H.; Murata, K.; Shigehara, K. *Chem. Lett.* **2010**, *39*, 168.

(11) (a) *Electronic Materials: The Oligomer Approach*; Müllen, K., Wegner, G., Eds.; Wiley-VCH: Weinheim, 1998. (b) Martin, R. E.; Diederich, F. *Angew. Chem., Int. Ed.* **1999**, *38*, 1350. (c) Segura, J. L.; Martín, N. *J. Mater. Chem.* **2000**, *10*, 2403.

(12) (a) Beginn, C.; Gražulevičius, J. V.; Strohriegl, P. *Macromol. Chem. Phys.* **1994**, *195*, 2353. (b) Paliulis, O.; Ostrauskaite, J.; Gaidelis, V.; Jankauskas, V.; Strohriegl, P. *Macromol. Chem. Phys.* **2003**, *204*, 1706. (c) Sonttag, M.; Strohriegl, P. *Chem. Mater.* **2004**, *16*, 4736.

(13) (a) Zhao, Z.; Xu, X.; Wang, H.; Lu, P.; Yu, G.; Liu, Y. *J. Org. Chem.* **2008**, *73*, 594. (b) Hu, B.; Wang, Y.; Chen, X.; Zhao, Z.; Jiang, Z.; Lu, P.; Wang, Y. *Tetrahedron* **2010**, *66*, 7583.

(14) (a) Chen, C.-H.; Lin, J. T.; Yea, M.-C. P. *Tetrahedron* **2006**, *62*, 8564. (b) Song, Y.; Di, C.-a.; Wei, Z.; Zhao, T.; Xu, W.; Liu, Y.; Zhang, D.; Zhu, D. *Chem.—Eur. J.* **2008**, *14*, 4731.

(15) Drolet, N.; Morin, J.-F.; Leclerc, N.; Wakim, S.; Tao, Y.; Leclerc, M. *Adv. Funct. Mater.* **2005**, *15*, 1671.

(16) Kato, S.-i.; Shimizu, S.; Taguchi, H.; Kobayashi, A.; Tobita, S.; Nakamura, Y. *J. Org. Chem.* **2012**, *77*, 3222.

(17) (a) Goncalves-Conto, S.; Carrard, M.; Si-Ahmed, L.; Zuppiroli, L. *Adv. Mater.* **1999**, *11*, 112. (b) Chen, Y.; Yamamura, T.; Igarashi, K. *J. Polym. Sci., Part A: Polym. Chem.* **2000**, *38*, 90.

(18) (a) Miyaura, N.; Yanagi, T.; Suzuki, A. *Synth. Commun.* **1981**, *11*, 513. (b) Miyaura, N.; Suzuki, A. *Chem. Rev.* **1995**, *95*, 2457.

(19) (a) Sonogashira, K.; Tohda, Y.; Hagihara, N. *Tetrahedron Lett.* **1975**, *16*, 4467. (b) Sonogashira, K. *J. Organomet. Chem.* **2002**, *653*, 46. (c) Tykwinski, R. R. *Angew. Chem., Int. Ed.* **2003**, *42*, 1566.

(20) Masuda, N.; Tanba, S.; Sugie, A.; Monguchi, D.; Koumura, N.; Hara, K.; Mori, A. *Org. Lett.* **2009**, *11*, 2297.

(21) When lithium—bromine exchange between **17** with *n*-BuLi followed by the addition of iodine was employed, the formation of **24** was not observed instead **13** was obtained as a reductive compound.

(22) For negative effects of the presence of copper iodide, see: Gelman, D.; Buchwald, S. L. *Angew. Chem., Int. Ed.* **2003**, *42*, 5593.

(23) Sakamoto, J.; Schlüter, A. D. *Eur. J. Org. Chem.* **2007**, 2700.

(24) Hay, A. S. *J. Org. Chem.* **1962**, *27*, 3320.

(25) (a) McMurry, J. E. *Chem. Rev.* **1989**, *89*, 1513. (b) McMurry, J. E.; Lectka, T.; Riko, J. G. *J. Org. Chem.* **1989**, *54*, 3748.

(26) Frisch, M. J.; Trucks, G. W.; Schlegel, H. B.; Scuseria, G. E.; Robb, M. A.; Cheeseman, J. R.; Montgomery, J. A., Jr.; Vreven, T.; Kudin, K. N.; Burant, J. C.; Millam, J. M.; Iyengar, S. S.; Tomasi, J.; Barone, V.; Mennucci, B.; Cossi, M.; Scalmani, G.; Rega, N.; Petersson, G. A.; Nakatsuji, H.; Hada, M.; Ehara, M.; Toyota, K.; Fukuda, R.; Hasegawa, J.; Ishida, M.; Nakajima, T.; Honda, Y.; Kitao, O.; Nakai, H.; Klene, M.; Li, X.; Knox, J. E.; Hratchian, H. P.; Cross, J. B.; Bakken, V.; Adamo, C.; Jaramillo, J.; Gomperts, R.; Stratmann, R. E.; Yazyev, O.; Austin, A. J.; Cammi, R.; Pomelli, C.; Ochterski, J. W.; Ayala, P. Y.; Morokuma, K.; Voth, G. A.; Salvador, P.; Dannenberg, J. J.; Zakrzewski, V. G.; Dapprich, S.; Daniels, A. D.; Strain, M. C.; Farkas, O.; Malick, D. K.; Rabuck, A. D.; Raghavachari, K.; Foresman, J. B.; Ortiz, J. V.; Cui, Q.; Baboul, A. G.; Clifford, S.; Cioslowski, J.; Stefanov, B. B.; Liu, G.; Liashenko, A.; Piskorz, P.; Komaromi, I.; Martin, R. L.; Fox, D. J.; Keith, T.; Al-Laham, M. A.; Peng, C. Y.; Nanayakkara, A.; Challacombe, M.; Gill, P. M. W.; Johnson, B.; Chen, W.; Wong, M. W.; Gonzalez, C.; Pople, J. A. *Gaussian 03*, revision C.02; Gaussian, Inc.: Wallingford, CT, 2004.

(27) We cannot entirely rule out the possibility that the DFT calculations underestimate the planarity of **2**, **4**, and **10**.

(28) The λ_{onset} of 1,4-bis(phenylethenyl)benzene is bathochromically shifted relative to that of 1,4-bis(phenylethynyl)benzene. (a) Beeby, A.; Findlay, K.; Low, P. J.; Marder, T. B. *J. Am. Chem. Soc.* **2002**, *124*, 8280. (b) Lim, S.-H.; Bjorklund, T. G.; Bardeen, C. J. *J. Phys. Chem. B* **2004**, *108*, 4289.

(29) Asker, E.; Masnovi, J. *Acta Cryst. E* **2006**, *62*, 1133.

(30) Compounds **13** and **14** show the longest λ_{max} values of 346 and 353 nm, respectively. Therefore, the four *t*-Bu groups in the two carbazole moieties in **1**, **4**, **7**, and **10** appear to be responsible for the bathochromic shifts within 15 nm in their absorption spectra.

(31) Suzuki, K.; Kobayashi, A.; Kaneko, S.; Takehira, K.; Yoshihara, T.; Ishida, H.; Shiina, Y.; Oishi, S.; Tobita, S. *Phys. Chem. Chem. Phys.* **2009**, *11*, 9850.
(32) Ohkita, H.; Ito, S.; Yamamoto, Y.; Tohda, Y.; Tani, K. *J. Phys. Chem. A* **2002**, *106*, 2140.
(33) Wytko, J.; Berl, V.; McLaughlin, M.; Tykwinski, R. R.; Schreiber, M.; Diederich, F.; Boudon, C.; Gisselbrecht, J.-P.; Gross, M. *Helv. Chim. Acta* **1998**, *81*, 1964.
(34) Qvortrup, K.; Jakobsen, M. T.; Gisselbrecht, J.-P.; Boudon, C.; Jensen, F.; Nielsen, S. B.; Nielsen, M. B. *J. Mater. Chem.* **2004**, *14*, 1768.
(35) We note that the acetylenic spacers in **4**−**9** also cause the slight elevation of their HOMO levels relative to those of the corresponding **1**−**3**. This is not consistent with the results obtained by the CV, where the electron-accepting ability of the acetylenic spacers apparently decreases the donor potency. The reason for this finding is unclear at present.
(36) Although the HOMO and LUMO densities of **1** are found on the whole conjugated backbone, the experimental results strongly suggest the lack of effective π-conjugation between the two carbazole moieties. It is likely that the calculations overestimate the π-conjugative effect in **1**.
(37) Zhao and co-workers reported that the LUMOs of oligoyne-centered π-extended tetrathiafulvalenes are gradually localized as the acetylenic chain length increases, see: Chen, G.; Mahmud, I.; Dawe, L. N.; Daniels, L. M.; Zhao, Y. *J. Org. Chem.* **2011**, *76*, 2701.
(38) Thompson, A. L.; Ahn, T.-S.; Thomas, K. R. J.; Thayumanavan, S.; Martínez, T. J.; Bardeen, C. J. *J. Am. Chem. Soc.* **2005**, *127*, 16348.